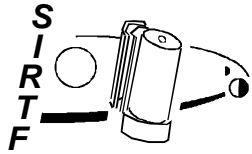


674-SN-100, Version 1.0



Space Infrared Telescope Facility

Science Requirements Document

3 February 1997

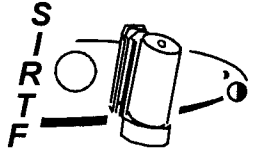
National Aeronautics and
Space Administration



Jet Propulsion Laboratory
California Institute of Technology
Pasadena, California

JPL D-14302

674-SN-100, Version 1.0



Space Infrared Telescope Facility

Science Requirements Document

Approved By

Responsible For

Larry Simmons 2/2/97

Larry Simmons
Project Manager

Michael Werner

Michael Werner
Project Scientist

3 February 1997

JPL D-14302

1	PURPOSE AND SCOPE.....	1
2	BROWN DWARFS AND SUPER PLANETS.....	3
2.1	Impact on Science.....	3
2.2	Previous Investigations.....	3
2.3	Measurements Required from SIRTf.....	5
3	PROTOPLANETARY AND PLANETARY DEBRIS DISKS.....	16
3.1	Impact on Science.....	16
3.2	Previous Investigations.....	17
3.2.1	Protoplanetary Disks.....	17
3.2.2	Planetary Debris Disks.....	17
3.2.3	The Outer Solar System.....	18
3.3	Measurements Required from SIRTf.....	18
3.3.1	Protoplanetary Disks.....	18
3.3.2	Planetary Debris Disks.....	24
3.3.3	The Outer Solar System.....	30
4	ULTRALUMINOUS GALAXIES AND ACTIVE GALACTIC NUCLEI.....	35
4.1	Impact on Science.....	35
4.2	Previous Investigations.....	36
4.2.1	What is The Link Between Ultraluminous Infrared Galaxies and Quasars?....	37
4.2.2	At What Redshift Do Heavy Elements Form?.....	38
4.2.3	What Are The Implications Of The Ultraluminous Galaxies For Galaxy Formation?.....	39
4.3	Measurements Required from SIRTf.....	39
5	THE EARLY UNIVERSE.....	46
5.1	Impact on Science.....	46
5.2	Previous Investigations.....	48
5.2.1	Galaxy Evolution and Star Formation in Galaxies.....	48
5.2.2	The Extragalactic Background Light.....	51
5.3	Measurements Required from SIRTf.....	51
	APPENDIX A.....	61
	REFERENCES.....	63

1 Purpose and Scope

The purpose of this document is to state the scientific requirements of the Space Infrared Telescope Facility - SIRTf. The approach taken to arrive at the requirements is to start with a set of clear scientific objectives of the SIRTf program as reviewed and endorsed by the National Academy of Sciences (Bahcall et al, 1991; Lanzerotti et al, 1994).

The four key SIRTf science objectives are:

- Search for and study of brown dwarfs and super planets,
- Discovery and study of protoplanetary and planetary debris disks.
- Study of ultraluminous galaxies and active galactic nuclei (AGN)
- Study of the early universe

Sample observation programs in each of these four scientific areas have been developed as examples of how SIRTf could be used to achieve these objectives. These programs are based on our current understanding of these astrophysical problems. They take advantage of the results of IRAS and COBE, and of the anticipated results of ISO, 2MASS and WIRE. Appendix A contains a brief summary of these and other missions and their relationship to SIRTf. It should be borne in mind that, while each of these other missions has its own unique characteristics, SIRTf will be so much more sensitive than any preceding or contemporary infrared facility that observations from SIRTf itself may be the best or only means of following up on many of SIRTf's scientific results. This is reflected in this document by such things as requirements for proper motion and position determination to facilitate this follow up.

The sample observational programs described in Sections 2 to 5 have been selected both to define and to delimit the measurement capabilities which SIRTf must provide. A mission which provides these capabilities will support a very wide range of astrophysical investigations, and this document should not be interpreted as describing the actual programs which will be carried out from SIRTf. The exact observations to be carried out on SIRTf will be defined and selected close to launch, and 75-to-80% of the observing time on SIRTf will be awarded to investigators selected from the broad scientific community.

For each element of the sample observation programs, a set of measurement requirements has been developed. They fall into the following categories:

- wavelength range,
- sensitivity,
- spectral resolution,
- spatial resolution,
- number of targets and amount of sky coverage.

These measurement requirements are tabulated at the end of each chapter. Thus the **requirements** which are imposed on SIRTf can be found in these four tables (Tables 2.2, 3.2, 4.1, and 5.1) which can be read independently of the accompanying text. These measurement requirements are combined with the mission constraints which include the usage of available

infrared detectors, performance of the launch vehicle, etc., to produce a set of derived design requirements. Examples of derived requirements are mission lifetime, telescope aperture size, instrument operating temperature, pointing stability and accuracy, etc. These derived design requirements are included in the SIRTf Level 1 requirements described in the SIRTf Program Plan.

2 Brown Dwarfs and Super Planets

2.1 Impact on Science

Our Milky Way Galaxy contains matter which is felt gravitationally but does not emit much visible light. A central goal of modern astrophysics is to identify the nature of this “dark matter.” One possibility is that there are large numbers of substellar objects (“brown dwarfs” or “Super Planets”) in the Milky Way – objects with masses less than $0.08 M_{\odot}$ ¹. Such objects do not have sufficiently high internal temperature and pressure to generate substantial amounts of energy by nuclear burning. Thus they are not true stars, but they radiate in the infrared as the heat generated in their formation diffuses outward from their interiors; because of this cooling, the brightness of a brown dwarf decreases as it ages. Because of their higher heat content, higher mass brown dwarfs are brighter than their lower mass cousins at the same age.

The basic goals of this program are to search the sky for brown dwarfs to determine whether they are important in the gravitational dynamics of the Milky Way, to provide constraints on the properties of dark, massive objects in the halo of the Galaxy, to search young clusters for recently formed brown dwarfs, and to look for “Super Planets” – substellar objects with masses between 0.001 and $0.01 M_{\odot}$ – orbiting the nearest stars. (For comparison, Jupiter, the most massive planet in our solar system, has a mass of $0.001 M_{\odot}$. It also has an internal heat source such as that described above and consequently radiates twice as much power as it receives from the sun.) Important additional scientific results will come from the observations of the low mass end of the main sequence which necessarily accompany any brown dwarf search.

2.2 Previous Investigations

The possible existence of brown dwarfs (stellar objects below the lowest mass possible for sustained nuclear fusion, $0.08 M_{\odot}$) has been talked about for years. Many experiments to detect such objects have been carried out and are on-going. Searches to date have concentrated on the more readily detectable high mass and/or young brown dwarfs. This creates a problem because such objects are difficult to distinguish from stars. Less work has been done on older and lower mass field brown dwarfs because of their faintness and low temperature. There are a handful of interesting candidates, but no acknowledged bona-fide field brown dwarfs have been located as of early 1996. On the other hand, convincing detections have been claimed for brown dwarfs and Super Planets in orbit around nearby stars. In particular, Gl 229 B has been measured at infrared and visible wavelengths (Nakajima et al, 1995) and has a luminosity of $5 \times 10^{-6} L_{\odot}$ and a most likely mass of $\sim 40 M_{\text{jupiter}}$ (Allard et al, 1996).

An alternate approach is to explore stellar clusters of known ages to search for brown dwarfs which formed coevally with the stars. Because the distances and ages of any brown dwarfs found in such an investigation would be known from the cluster properties, this technique permits

¹ M_{\odot} is one solar mass, 2×10^{33} gm

assessment of the physical models for these objects. Stauffer et al. (1989,1994), Rebolo et al. (1995) and Martin et al. (1996) reported the detection of faint, red objects towards the Pleiades cluster whose photometric characteristics were compatible with their being high mass brown dwarfs. Confirmation that at least three of these objects are indeed brown dwarfs has come recently from spectra obtained at the Keck observatory (Basri, Martin, and Graham 1995) which showed these stars pass the "lithium test" (i.e. they have nearly primordial lithium abundances, indicating that their central temperatures are less than 2.5 million degrees), a spectroscopic brown dwarf criterion proposed by Rebolo et al. (1992) and Magazzu et al. (1993).

A particularly noteworthy recent development concerning Super Planets has been the detection of planets with masses about that of Jupiter around nearby stars, starting with the work of Mayor and Queloz (1995) and Marcy and Butler (1996) and Butler and Marcy (1996). A recent summary by Burrows et al (1996) lists nine planetary companions of nearby stars, all more massive than $0.5 M_{\text{Jupiter}}$, and five more massive than $\sim 2.5 M_{\text{Jupiter}}$. The rate of discovery of these companions is accelerating, and it is now clear that such Super Planets must be fairly common around nearby stars. This gives extra impetus to SIRTf's attempts to identify them – whether by studies of field stars, of young clusters or by exploring the nearest stellar systems.

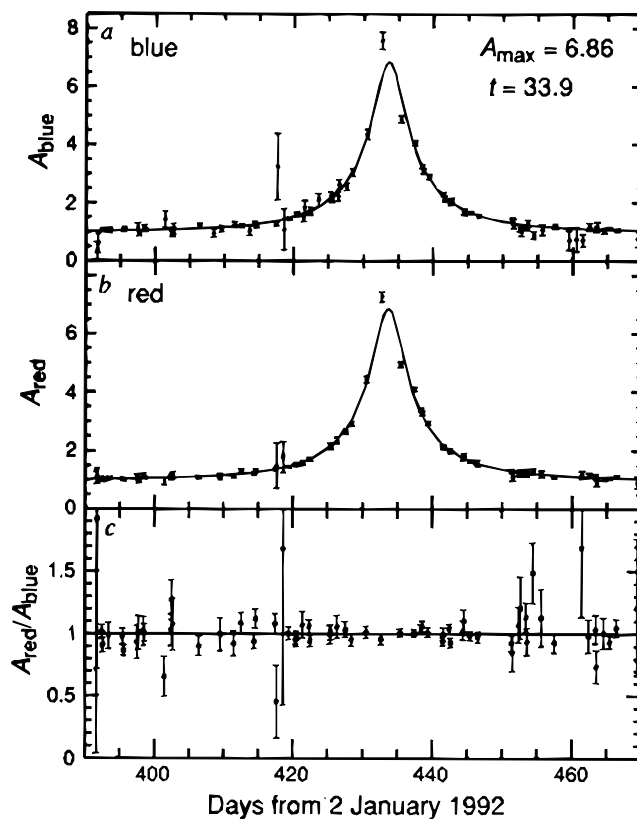


Figure 2.1. - Light curve showing apparent brightness vs. time of a distant star for which the brightness is temporarily amplified by gravitational lensing produced by a MACHO moving across our line of sight to the star.

The search for low mass brown dwarfs is related to the question of the unseen mass of the Milky Way. It has been known for a number of years that most of the mass of the Galaxy is in the form of a massive halo of unknown composition that does not produce much visible light (see, for example, Bahcall, Schmidt & Soneira 1982). The mass of the dark halo is about 90% of the total mass of the Galaxy. This unseen material has a different spatial and kinematic distribution than the bulk of the obvious bright stars and might be detected by its distinctive qualities. The recent detection of candidate MACHO (MASSive Compact Halo Object) gravitational lensing events using background stars in the LMC (Figure 2.1, Alcock, et al, 1993) allows us to infer the presence of low mass objects in the halo and to address the possibility that most of the mass of the Milky Way is in very low mass objects, perhaps very old brown dwarfs. The mass of the lensing MACHO is indicated by the time-scale of the event. Since lensing cross section is proportional to mass, the time scale will be proportional to the square root of mass and inversely proportional to the transverse

velocity. To date, the reported events have ranged in time scale from about 1 month to more than 2.5 months indicating masses from roughly $0.1 M_{\odot}$ to $1.0 M_{\odot}$ with a lower limit possibly as low as $0.01 M_{\odot}$ (Evans & Jijina 1994, Alcock et al 1996). Gould (1994) has shown how a satellite at a distance of a few tenths of an astronomical unit from the Earth can provide valuable data for the determination of the MACHO mass.

2.3 Measurements Required from SIRTf

SIRTf's program for the study of brown dwarfs and Super Planets should have the following major elements:

Program 2.1 – A search for halo brown dwarfs

Program 2.2 – MACHO parallax studies

Program 2.3 – Cluster brown dwarfs and the low mass main sequence

Program 2.4 – Spectroscopy of brown dwarfs

Program 2.5 – Superplanets around nearby stars

Program 2.1 - A search for halo brown dwarfs

Based on a long-term, ground-based proper motion survey, Dahn et al. (1994) showed that ordinary stars account for at most 1/150 of the inferred dynamical mass of the halo. Recent HST observations led Bahcall et al. (1994) to also conclude with some certainty that red dwarfs can not constitute a major mass fraction of the halo of the Galaxy (see also Graff and Freese 1996 for a reanalysis of these data). However, it is now known that compact microlenses (MACHO's) exist in our halo (Alcock et al. 1993). One consequence of the HST observations is that if the halo is indeed made of MACHO's, they are not main sequence stars above the hydrogen-burning mass limit. Based on estimates that the median mass of the microlensing sources is of order a few tenths of a solar mass (Alcock et al. 1996; De Paolis et al, 1996, Jetzer 1994), white dwarfs have been proposed as being the dominant component of the halo missing mass. An initial calculation indicates that very low mass objects (masses from 0.001 to $0.03 M_{\odot}$.) make up at most 20% of the dynamically inferred halo mass. Thus the preliminary results are still consistent with a significant brown dwarf component. SIRTf must be able to detect these objects and to determine their space density, which would be impossible to achieve with ground-based observations.

The halo material will be spatially intermingled with that of the galactic disk in the solar neighborhood (although distinguishable by its motion, as discussed below), so SIRTf can search locally for brown dwarfs. In order to derive measurement requirements for such a search, we have to assume some parameterization for the mass function. Based on the mass function for halo stars (Dahn et al. 1994), it is clear that a population of halo brown dwarfs which makes up a significant fraction of the dynamical mass of the halo cannot be a simple extrapolation of the stellar mass function. There needs to be a significant enhancement in the mass function beginning near the hydrogen burning mass limit, presumably indicating a separate mode of formation for substellar objects. In order to provide a "significant" mass in brown dwarfs (say 10% of the dynamical halo mass), this mode would have to be peaked at a few hundredths of a solar mass and have a fairly narrow mass range. While such a distribution does not seem a priori likely, there are arguments which can be advanced in its favor. First, an enhancement in the mass function for the halo at $0.05 M_{\odot}$ has in fact been predicted (Salpeter 1992) based on the expected properties of low mass, low

Z protostars. Second, given the quite small area surveyed to date, the detection of three brown dwarfs in the Pleiades indicates that the mass function in that cluster apparently does turn up near the hydrogen burning mass limit (Martin et al. 1996). Third, ANY stellar explanation of the halo missing mass may require a seemingly odd mass function – the white dwarf explanation requires a very peaked mass function, since too many high mass stars violates galactic metallicity constraints whereas too many low mass stars would violate the measured mass density of main sequence stars in the halo (Alcock et al. 1996; Adams and Laughlin 1996; Chabrier et al. 1996).

There are a variety of strategies for SIRTF searches for halo brown dwarfs. One possible approach is discussed below. It involves a large area survey and identification of candidate brown dwarfs by a subsequent survey searching for high proper motion objects. For specificity, we assume a log-normal distribution for the sub-stellar component of the halo, as proposed by Han and Gould (1996) in their modelling of the MACHO events towards the galactic bulge. That is, the assumed functional form is:

$$N(x)dx = Ke^{-\frac{1}{2\sigma^2} \left(\frac{x - \langle x \rangle}{\sigma} \right)^2} dx$$

where K is a constant, and $x = \log M$, where M is the brown dwarf mass in solar units.

We do not choose the same parameters ($\langle x \rangle = -1.12$, $\sigma(x) = 0.57$) for the log-normal distribution as Han and Gould found for the bulge, since a distribution with those parameters would violate the constraints imposed by the stellar census of the halo (Dahn et al. 1994) if more than 1% of the dynamical halo mass were in this mode. Instead, we assume that the difference in composition and initial conditions allows the halo substellar mass function to be shifted to lower masses - $\langle x \rangle = -1.55$ and $\sigma(x) = 0.30$. For normalization, we assume that 10% of the dynamical mass of the halo is in this component (equivalent to $0.0086 M_{\odot}/pc^3$). With these parameters, this component does not violate the constraint imposed by the Dahn et al. survey of halo stars (or the HST WFPC survey), and it also is easily consistent with the limits imposed upon substellar objects by the MACHO surveys.

In order to determine the expected results from a survey for halo brown dwarfs with SIRTF, we must first consider the expected brown dwarf fluxes at SIRTF wavelengths and the target SIRTF sensitivities. Below, we display the predicted fluxes from brown dwarfs with ages of 10^{10} yr, assuming the theoretical model calculations of Nelson et al (1986) – very similar numbers would be predicted using the Burrows et al. (1993) models – and a black-body spectrum. The approximation of a black body emission from a brown dwarf is almost certainly not appropriate for the brown dwarfs we might find in this deep survey, and it is probably fair to say that we know relatively little about the emergent flux from brown dwarfs and so should keep an open mind. The brown dwarf companion to GL229B, for example, shows excess emission at $5 \mu m$, similar to what is seen from Jupiter (Nakajima et al. 1995); this signature, if persistent, could be an important component of a SIRTF survey and survey follow-on strategy.

Table 2.1 Fluxes from Old Brown Dwarfs that are 10 pc from the Sun

Mass [M_{\odot}]	Radius [R_{\odot}]	Temp [K]	F(2.2 μm) Jy	F(3.5 μm) Jy	F(4.5 μm) Jy	F(6.5 μm) Jy	F(8 μm) Jy
0.06	0.83	750	6.7(-5)	4.4(-4)	7.5(-4)	9.1(-4)	8.6(-4)
0.03	0.01	450	2.9(-7)	1.7(-5)	6.5(-5)	1.8(-4)	2.3(-4)
0.01	0.12	225	2.1(-13)	1.3(-9)	7(-8)	1.9(-6)	6.1(-6)
SIRTF target 85 cm 10 σ 150s				9.3(-6)	1.2(-5)	6.6(-5)	1.1(-4)

The table shows that SIRTF would have to achieve its target sensitivities to detect brown dwarfs as low in mass as 0.03 solar masses in short integrations; we see that the optimum wavelength for detection of objects in this mass and age range is in fact 4.5 μm . The brown dwarf large area survey would be carried out in a step-and-integrate mode. A good approach would be to take three dither steps per frame in the scan direction of the survey. A given source can be prevented from appearing on the same row of the array at each dither step by rotating the arrays in the SIRTF focal plane by a few degrees with respect to the line joining the arrays. The final optimization of dither pattern would depend on the detailed characteristics of the SIRTF attitude control system.

A detailed strategy for such a program from SIRTF relies on 10- σ detection of brown dwarfs at 4.5 μm , and identification of candidates through their proper motion in a second survey about two years after the first. A reasonable survey goal would be to identify ~ 50 brown dwarf candidates from their proper motions. Assuming $>50\%$ verification of such candidates, this would allow determination of the brown dwarf abundance with $\sim 20\%$ precision. Such a survey would require observing ~ 300 sq. degrees to sensitivity levels about those given in Table 2.1

A major problem will be to sort out the halo brown dwarfs from all the other objects found in the survey; the positive identification of a brown dwarf is a challenge. Most of the infrared bright objects in the sample will be quasars and galaxies. Although we do not know the infrared spectra and source counts of these extragalactic objects with high precision, as a first estimate we assume that there might be $\sim 10^7$ extragalactic sources in the same field where we might detect a total of ~ 100 brown dwarfs. Therefore, the task will be to separate the candidate brown dwarfs from the extragalactic objects.

One possible way to do this would be to look for objects with high proper motions. The first survey could be followed up approximately two years later with follow up observations aimed at identifying high proper motion objects, because a straightforward way to separate brown dwarfs from extragalactic objects is by their proper motions. Note that the second survey need not cover the entire area covered by the first, but could be targeted at brown dwarf candidates selected from the first survey by their brightnesses and spectral energy distributions (which can be determined both from the infrared images alone and from comparison with optical images). If the halo objects are not participating in the rotation of the disk, then we can expect that the transverse velocities of the brown dwarfs range from 200 to 400 km/s. If we assume a transverse motion of 300 km/s, and that a second SIRTF survey would allow us to measure proper motions of 2" over a two-year time base, then we should be able to identify brown dwarfs via their proper motions out to a

distance of 65 pc. The survey described above includes about 45 brown dwarfs out to this distance.

Once candidate brown dwarfs are identified, it will be necessary to measure their temperatures, and, if possible, their distances through trigonometric parallax. Once we have an estimate of their mass and the space density of these stars, we will be able to determine their importance for the gravitational dynamics of the Milky Way Galaxy. Ideally, we would like a trigonometric parallax to demonstrate that the object has low luminosity. But even in the absence of a known parallactic distance, there should be little ambiguity as to whether the object is a true brown dwarf. According to the models, the lower mass brown dwarfs have temperatures less than 500 K, and observations in several wavelength bands ought to be able to identify such objects. Any object outside the Solar System with a temperature lower than 500 K and a proper motion greater than 1" per year almost certainly is a brown dwarf.

Subsequent followup spectroscopy from SIRTf of the brighter examples would greatly increase our detailed understanding of these objects, as discussed in detail in Program 2.4 below. Given the assumed density of brown dwarfs, the nearest such objects detected in a 300 square degree sample should be about 15 pc distant from the Earth. SIRTf's low resolution spectrometer must be capable of obtaining a spectrum of such an object in a long integration.

Program 2.2 - MACHO parallax studies

Current studies of gravitational microlensing from MAssive Compact Halo Objects (MACHOs) are conducted from the Earth and can measure only the peak amplification, which gives the ratio of the impact parameter to the Einstein ring radius, and the time scale, which gives the ratio of the Einstein ring radius to the transverse velocity of the MACHO. The quantity of greatest interest, the Einstein ring radius, which gives the mass of the MACHO, can only be estimated statistically from the Earth based observations, using assumptions about a typical transverse velocity. However, if observations can be made from other stations separated by a few tenths of the Einstein ring radius, more parameters can be determined. If only two stations are available a four-fold ambiguity remains in the transverse velocity which can be used for statistical studies of the MACHO mass and distance or to actually measure the mass and distance if the ambiguous velocity solutions can be eliminated as producing unlikely or impossible values of mass or distance. A typical Einstein ring radius is 0.3 au, so the stations need to be separated by a few tenths of an au, which favors a SIRTf in a solar orbit.

SIRTf could serve as a remote MACHO observatory by treating MACHOs as targets of opportunity. An Earth based observatory would announce the occurrence of a large amplitude lensing event, then SIRTf would observe the lensed star as the lensing event proceeds. Fortunately the LMC is at the South ecliptic pole and can always be accessible to SIRTf. These measurements require a telescope able to measure the brightness of the 19th magnitude stars being monitored by the MACHO project. This is 9 μ Jy at 3.5 μ m. Such an exposure would be desired once every 2 days or so for each active lensing event for the several tens of days that the event lasts. These targets of opportunity might become available as often as once per month.

Program 2.3 - Cluster Brown Dwarfs and the Low Mass Main Sequence

A complement to looking for halo brown dwarfs is to study the very low mass end of the initial mass function (IMF), that is the fraction of stars formed as a function of mass. Knowledge of the low mass end of the IMF will help to indicate whether or not current star formation rates could have provided enough brown dwarfs to be a dynamically significant mass reservoir, and observation of individual low mass objects will provide information as to what brown dwarfs actually look like. Most studies of the IMF have concentrated on field stars (e.g. Scalo 1986, Basu and Rana 1992, Tinney 1993). Because substellar objects will have faded to relative invisibility by the time they are as old as typical field stars, these studies have been unsuccessful in obtaining any information about the IMF below about $0.1 M_{\odot}$ and, in fact, are subject to significant uncertainties and disagreements even for low mass stars on the main sequence. An extended survey for brown dwarfs in the general field such as that described above would, as a by-product, produce a much improved definition of the low mass end of the main sequence.

An alternate, better-controlled approach which SIRTf is well-equipped to pursue is to study the IMF in regions where we might expect to find young brown dwarfs. There are two places one might look, open clusters such as the Pleiades, and very young clusters in recently or currently active star formation regions. This method has the advantage that the low mass stars and brown dwarfs, if any, that formed with the cluster should still be in the cluster, so one knows where to point a telescope to look for them. Also, cluster brown dwarfs will be, on the average, younger than their halo counterparts and therefore hotter, more luminous and easier to detect. In addition all the stars of the cluster will be the same age so the age of any brown dwarfs will be known.

Open clusters

Nearby open clusters are best searched for brown dwarfs at relatively short wavelengths ($0.5 - 8 \mu\text{m}$) where they are predicted to be brightest. However a method is still needed to sort out the faintest, reddest cluster members from the background. Traditional methods of determining cluster membership, measurement of proper motion or use of photometry for initial selection followed by confirming spectroscopy, are not easily applicable to the faintest cluster members. A particularly useful technique for selecting faint cluster members based on photometry only has been to sort stars in a color-magnitude diagram. The faintest open cluster brown dwarf candidate identified solely from optical imaging, PPl 15 in the Pleiades, has recently been confirmed as a brown dwarf or transition object based on the detection of lithium in its spectrum (Basri, et al 1995). Measurements in the V, I and K bands from ground based telescopes have allowed identification of candidate Pleiades cluster members down to masses of 0.05 to $0.04 M_{\odot}$ (Williams et al. 1996). Extension of this technique to 0.02 and $0.01 M_{\odot}$ requires sensitive observations at wavelengths longer than K band because these low mass objects have become too faint for detection at V and the I-K, or other near infrared colors, do not provide enough selectivity against more massive objects. SIRTf should therefore provide measurements at wavelengths out to $8-12 \mu\text{m}$ with enough sensitivity to detect ~ 0.01 solar mass objects in the nearest several open clusters (up to 140 pc distance). This provides enough wavelength coverage to cover the likely peak in the spectral emission from such objects. The clusters to be studied have angular scales of several square degrees. Programs have been approved for ISO to search for

Pleiades and Hyades brown dwarfs in the $0.02 M_{\odot}$ mass range. SIRTf should be able to extend any ISO results to other clusters and lower masses. Part of the utility of detection and measurement of cluster brown dwarfs will be to develop accurate brown dwarf signatures to aid in selecting brown dwarf candidates from a halo survey.

Embedded clusters

Our ability to detect brown dwarfs is greatly enhanced if we can find very young ones, when they are still relatively luminous, as might be expected in very young clusters still embedded in regions of recent or current star formation. A particularly felicitous stage for such investigations is the period when the brown dwarf is between a million and a few million years old, when it is burning deuterium and is therefore in a relatively stable configuration. The difficulty in identifying brown dwarfs at this stage is that they are likely still to be embedded in the interstellar clouds of dust and gas from which they formed, so that means must be found to disentangle the effects of extinction and deduce the intrinsic source properties.

A way to study low luminosity embedded sources is to obtain multi-band photometry of them and to correct their observed properties for reddening until the deduced intrinsic properties agree with theoretical isochrons that predict the temperature and luminosity as a function of mass and age. This procedure is still at a rudimentary stage, but as spectroscopy becomes available for favorable sources and as theoretical atmospheric calculations are improved both from better input physics and in response to observational results, the method should become very powerful as a means to estimate the masses of embedded sources. The methods will be effective only where the embedded source has been measured at enough wavelengths that the problem of correcting the extinction is over constrained; in this case, there is enough information to provide an internal consistency check. Large groundbased telescopes have adequate sensitivity to obtain photometry of young brown dwarfs in the nearest embedded clusters only between 1 and $2.5 \mu\text{m}$. The addition of longer wavelengths will provide the necessary constraints and checks on the fits and furthermore will strongly constrain the overall photospheric emission of the sources because the entire spectral range over which brown dwarfs can emit significant power will be measured.

SIRTf observations in the 3 to $30 \mu\text{m}$ region must be able to play a central role in defining the faint end of the main sequence in clusters, identifying young brown dwarf candidates and following up with spectroscopic confirmation of the candidates. As the techniques for fitting the photometry are refined, it should also be possible to isolate sources that are too faint for spectroscopy but which are extremely likely to be additional brown dwarfs. A cluster brown dwarf search can be carried out most efficiently from SIRTf using a short wavelength camera to survey nearby clusters at wavelengths between 3.5 and $8 \mu\text{m}$. These are the most sensitive bands for detection of brown dwarfs with masses greater than $0.02 M_{\odot}$ and are adequate to detect $0.01 M_{\odot}$ objects. Follow on observations at $24 \mu\text{m}$ could be important for supplementing the data on the lowest mass objects.

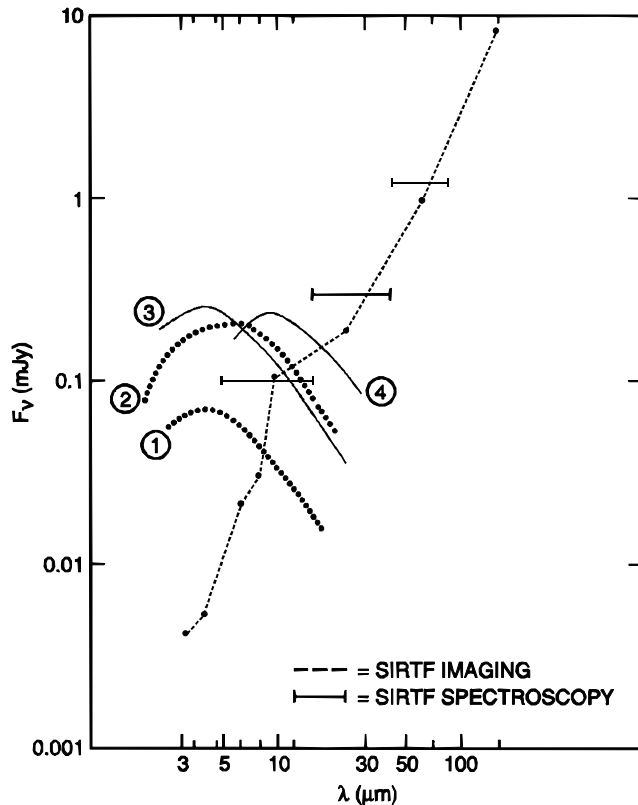


Figure 2.2. - Predicted brightness of brown dwarfs compared with the SIRTf sensitivity targets for photometry (5σ , 500 sec) and low resolution spectroscopy (5σ , 10000 sec). The objects shown are:

a 0.02 solar mass object in the Hyades cluster [distance = 48 pc, age = 6.6×10^8 yr]; a 0.01 solar mass object in the Ophiuchus star forming region [distance = 170 pc, age = 10^6 yr], with its flux reduced (by an order of magnitude at $2\mu\text{m}$) due to absorption by dust in its immediate environment; a 0.04 solar mass object in the Pleiades cluster [distance = 125 pc, age = 78×10^6 yr]; and a 0.03 solar mass, 1×10^{10} yr old field brown dwarf at a distance of 10 pc from the sun.

subject to heavy near infrared extinction by the dust clouds within which they formed. This capability is thus an essential complement to the photometric search procedures described above.

We summarize the measurement requirements by showing in Figure 2.2 the predicted brightness – based on the models of Nelson et al – for low mass brown dwarfs in the Hyades cluster [distance = 48 pc, age = 6.6×10^8 yr], in the Pleiades cluster [distance = 125 pc, age = 78×10^6 yr] and in the Ophiuchus star forming region [distance = 170 pc, age = 10^6 yr], compared with the SIRTf target sensitivity levels. Also shown is the predicted brightness of an old 0.03 solar mass brown dwarf at 10 pc from the sun (see Table 2.1).

Program 2.4 - Spectroscopy of brown dwarfs

Following the completion of the surveys, spectroscopic followup of the brightest candidates should be carried out to confirm the identification and to improve our understanding of the properties of substellar objects. The results of Marley et al (1996) on the brown dwarf candidate Gl229B show an atmosphere with strong molecular absorption feature of water and methane out to $5\mu\text{m}$, and predict additional features due to water, methane, and ammonia between 5 and $15\mu\text{m}$ (Figure 2.3). Cooler objects which may be accessible only to longer wavelength spectroscopy can thus be expected to reveal a variety of molecular and possibly solid material in their atmospheres. The understanding obtained from these spectral investigations can also be used to refine the strategy adopted for the halo brown dwarf survey described above. In addition, the longer wavelength spectroscopy will be valuable for the study of young substellar objects which may be

As is clear from Figure 2.3, low resolution spectroscopy will be appropriate for the classification and characterization of the substellar objects at wavelengths from 5 – 15 μm , although higher resolution might be used in subsequent searches for trace constituents and non-equilibrium molecular emission. In either case, location of these targets and placement on the spectrograph slits would require either a precise positional determination from SIRTf or a peak-up mode which can be used to locate faint sources in crowded and complicated fields.

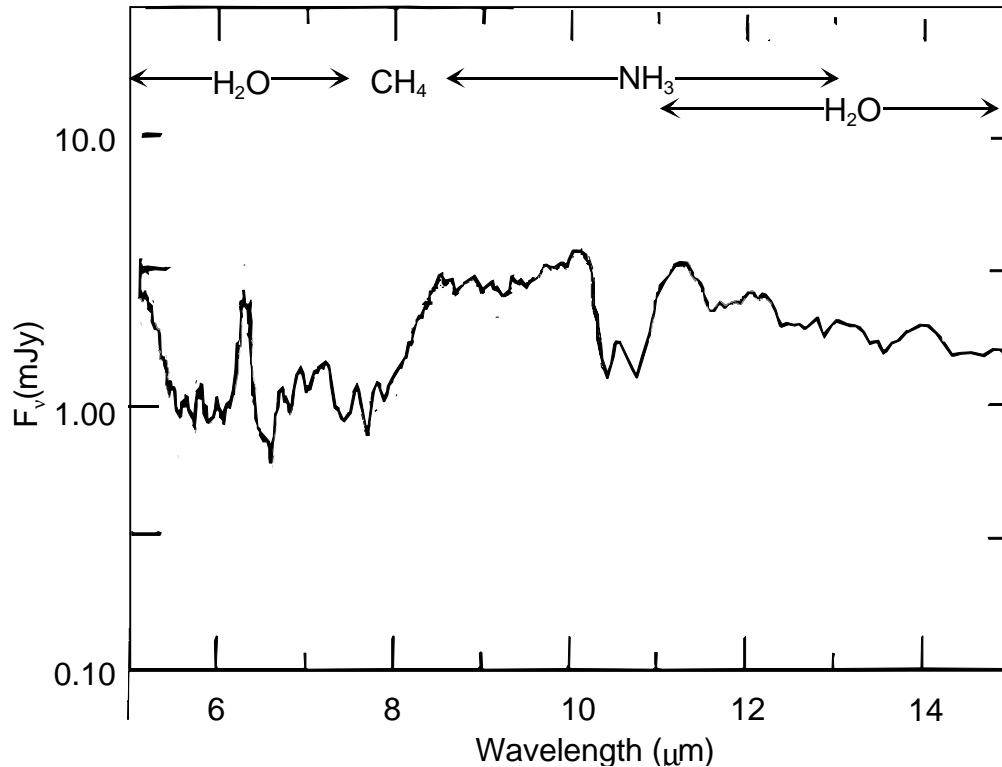


Figure 2.3 The predicted 5-15 μm spectrum of the brown dwarf Gl229B, adapted from Marley et al (1996). To study a range of such objects, SIRTf must be able to obtain spectra over this wavelength interval with resolving power ~ 50 and sensitivity ~ 0.1 mJy.

Program 2.5 - Super-Planets around nearby stars

An important component of our Brown Dwarf-Super Planet program is to search for low mass ($< 0.01 M_{\odot} = 10 M_{\text{Jupiter}}$) companions to the nearest stars. Although self-luminous like brown dwarfs, such objects might be referred to as Super-Planets, and understanding their properties and prevalence would improve our understanding of the formation of planets and planetary systems. Super Planet companions have now been reported associated with about a half dozen nearby, solar type stars [see summary in Burrows et al, 1996]. These have been found largely by reflex velocity measurements most sensitive to small planetary orbits. Nevertheless, the fact that planets more massive than Jupiter have been found in orbits smaller than the Earth's has confounded our theoretical expectations and indicates that we have much to learn about planetary system architecture, formation, and evolution.

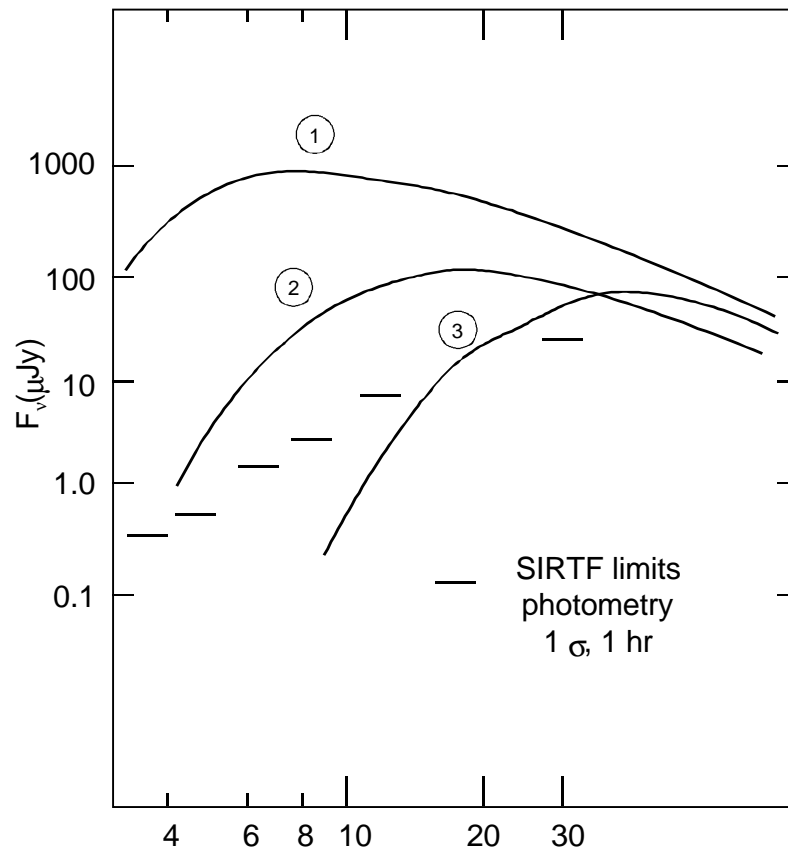


Figure 2.4 - Predicted spectral energy distributions for 1 and 5 Jupiter mass superplanets at distances of 3-to-10 pc from the Earth, with ages between 0.1 and 4.5 GYr..SIRTf's sensitivity target for imaging [1s, 3600 s] is shown. The specific predictions are: #1 - a 5 Jupiter mass object, age = 0.1 Gyr, d= 10pc; #2 - a 5 Jupiter mass object, age =1Gyr or a 1 Jupiter mass object, age = 0.1 Gyr, d=10pc; #3 Jupiter itself, age = 4.5 Gyr, d = 3pc

because they have more internal heat. If SIRTf can achieve the sensitivity targets shown in Figure 2.4, there is a large volume of search space in which SIRTf should be able to find superplanets, because there are some 300 stars within ~10 pc of the sun. Note that Jupiter itself would be detectable beyond 3pc in a long integration. To extend the observations beyond 8 μ m in cases where the planet lies within ~2" of the star [~10au, the radius of Saturn's orbit, for a star at a distance of 5pc] it would be necessary to carry out super resolution measurements from SIRTf at ~24 μ m which would use the shorter wavelength morphology as the deconvolution template.

Because of the low contrast with the nearby central star, angular resolution, stable detectors, and stable images allowing super resolution will be at a premium. At 10 pc the SIRTf beam should have a scale of 20 au making SIRTf measurements sensitive to companions with orbital radii comparable to the size of the outer solar system (20 to 100 au); this translates to a beam size ~2". As emphasized above, this nicely complements the radial velocity techniques which

SIRTf can contribute uniquely in this area by the study of Super Planets at larger distances from their parent stars, objects too distant to produce a detectable radial velocity signature but which will be visible in the infrared due to their self-emission. Just as the extra-solar planets discovered to date lie much closer to their parent stars than Jupiter does to the Sun, SIRTf's observations will be uniquely valuable even in cases where they are most sensitive to objects lying at larger orbital radii than Jupiter. In Figure 2.4, adapted from Burrows et al (1996), we show the predicted flux from objects of masses 1 and 5 M_{Jupiter} and ages = 0.1 to 4.5 Gyr which are in orbit around solar-type stars at distances of 3–10 pc from the Earth. Note that the radiation from the superplanets in these cases results from their internal energy source, not from the heating effect of the star. Older superplanets are fainter because they have had longer to cool; massive ones are more luminous

have recently identified Jupiter-mass planets orbiting several nearby stars, but in much smaller, higher velocity orbits.

A comprehensive SIRTf program should survey the 40 stars within 5 pc and a selection of another 60 stars – chosen to fill gaps in spectral type, age, multiplicity, luminosity class, etc. – within 10 pc for a total sample of 100 stars. The sample must be observed both at the beginning and towards the end of the mission so that suspected companions could be confirmed by their proper motion, which will be the same for the star and its companion. This motion must be discernible by SIRTf during its operational lifetime. For a typical stellar velocity of 30 km/s, a star at a distance of 10pc, and a two-year measurement interval, the accumulated motion of the two bodies is ~ 1.2 arcsec relative to the background star field at 3.5 and 8 μm : the relative motion of the star and its Super Planet companion would of course be much less than 1.2 arcsec.

Table 2.2 Science Requirements for the Brown Dwarfs and Superplanets Program

Program	Wavelength Range (μm)	Sensitivity Required	Spectral Resolution ($\delta\lambda/\lambda$)	Spatial Resolution (arcsec)	# of Targets	Comments
2.1 - Brown Dwarf Survey	3.5 - 8 μm	9 μJy (3.5 μm) to 110 μJy (8 μm) all 10σ (see table 2.1)	~ 0.25	$\sim 2''$ for proper motion studies	~ 300 square degrees; target is ~ 50 brown dwarfs within ~ 65 pc	detect $0.04M_{\odot}$ brown dwarf at 45 pc, proper motion follow up; detect $2''/2$ yr
2.2 - MACHO Parallax	3.5 μm	9 μJy - 10σ	~ 0.25	$\sim 2''$	Targets of Opportunity - lasts \sim one month	Expect targets as often as once per month
2.3 - Cluster Low Mass Luminosity Function	3.5 - 24 μm	25 μJy , 3.5/ 4.5 μm ; 50 μJy , 6.3/8 μm ; 100 μJy , 24 μm [all 5σ]	~ 0.25	$\sim 2''$	7 clusters, sizes from ~ 1 to ~ 25 sq degree	Survey goal to detect 0.01 solar mass objects at 5σ level from 3.5-8 μm ; follow up at 24 μm on cool candidates
2.4 - Spectroscopic Follow of 2.1 & 2.3	5 - 15 μm	100 μJy , 5σ , per resolution element	~ 0.02	size slit for resolution, sensitivity	25 targets from surveys 2.1 & 2.3	Selection of candidates from cluster and field surveys; need to place targets on slits with $< 1''$ precision
2.5 - Nearby Star Survey for Superplanets with $M < 10$ Jupier Mass	3.5 - 24 μm	6,6,15,25,75 μJy @ 3.5,4.5,6.3,8,24 μm , all 10σ	~ 0.25	$\sim 2''$ to separate planet at 20 au from star at 10pc	~ 100 stars	Observe all stars within 5 pc and some between 5 & 10 pc; super resolution at 24 μm ; proper motion follow up (1.2''/2 yrs)

3 Protoplanetary and Planetary Debris Disks

3.1 Impact on Science

Speculation about the existence of planets and life around other stars has fascinated humanity for centuries. It is believed that the formation of stars and planetary systems begins with minor density enhancements in the interstellar medium and accelerates through successive stages of collapse and fragmentation, ending with the emergence of a newly-formed star out of the cocoon of dust and gas within which it was born. Even at this stage, however, similar formation and evolution processes may be occurring within a protoplanetary disk ringing the now visible star. Condensing planetesimals attempt to grow by capturing the protoplanetary material in competition with dissipative processes – collisions, evaporation, and outflow – which tend to drive the material away from the star.

This process of star and planetary system formation out of interstellar gas and protoplanetary disks is of central importance for astrophysics. Many of its major phases are uniquely accessible to observations at infrared wavelengths. The condensation and collapse occurs within dense clouds which are impenetrable to optical and ultraviolet radiation. Particularly at its earliest stages, the protostellar material is at such low temperatures that it radiates only in the infrared. Circumstellar disks within which planets may be forming can be discovered in the infrared as they reradiate the power absorbed from the central star. Furthermore, at the various stages of disk evolution, spectroscopic investigations in the infrared provide unique information about the composition and conditions of the protoplanetary material.

Even when the process of planetary formation is completed, it may leave behind a persistent residue in the form of a tenuous planetary debris disk which is replenished by continued collisions among cometary and asteroid-sized objects. The discovery of such debris disks - again visible by their infrared radiation - around nearby solar-type stars can provide evidence for the existence of planetary systems around many stars other than the sun. Spectra of comets in the outer Solar System can be compared with spectra of the protoplanetary disks and the planetary debris disks to determine whether the material from which planets may have formed around nearby stars is similar to that from which our own planetary system condensed. Finally, infrared photometry of distant Kuiper Belt objects within our Solar System can allow detailed dynamical and structural comparisons between the solar system and the similar systems around other stars, helping evaluate our inferences about extra-solar star and planetary formation processes.

The goals of this program are: 1) to characterize the properties of potentially planet-forming disks associated with young stars and to determine how the properties depend on the mass, age, and other characteristics of the central star; 2) to study the character of planetary debris disks around mature, solar-type stars in order to understand their -significance as potential indicators of macroscopic bodies - from cometary nuclei to planets - which might be orbiting the same stars; and 3) to compare the origin, composition, and properties of extra-solar debris disks with those of the various dust components of our own solar system. The scientific advances which SIRTf makes in pursuit of the second and third goals will also support the planning for extra-solar planet searches such as those being carried out under NASA's Origins program.

3.2 Previous Investigations

3.2.1 Protoplanetary Disks

A very active area of research is the mapping of star formation regions in the near infrared (1–2.5 μm), where surveys can provide a count of all the stars in a forming cluster. By the time SIRTf flies, a full survey of the sky (2-MASS) will be available from 1–2.5 μm . At longer wavelengths, data from IRAS and from Earth-based telescopes have identified a number of candidate protostars, and additional candidates will be found by ISO. The energy distributions of a subset of these objects have been interpreted as indicative of protoplanetary disks, but the character and geometry of these proposed disks is still highly uncertain, and a much larger sample of objects in a variety of evolutionary stages must be investigated.

A number of nearby systems with dramatic disks appear to be young stars fully emerged from their parental clouds, but with the protoplanetary disks still in the process of clearing. Examples include HD 98800 (Grogorio-Hetem et al. 1992; Fekel & Bopp 1993), HR 4796B (Jura et al., 1993; Stauffer, Hartmann, & Barrado Y Navascues 1995), and possibly Beta Pic (Lanz, Heap, & Hubeny 1995). These unusual objects may represent a short-lived transitional stage between the protoplanetary disks and the debris disks.

3.2.2 Planetary Debris Disks

IRAS inaugurated this field of study by revealing planetary debris systems in orbit around nearby solar-type stars such as Vega, Fomalhaut, and Beta Pictoris. These debris disks detected around main-sequence stars consist of swarms of 1–100 μm -sized particles that probably originate from collisional comminution of planetesimals (a few meters to a few hundred kilometers) left over after star (and planet) formation. It appears that the disks lie in the zone approximately 50–200 astronomical units from the star, and mostly confined to the stellar equatorial plane. The particles thought to constitute these disks will not survive for times as long as the stellar lifetimes; thus their presence around these stars at the current epoch requires that their parent bodies – asteroids, comets, planetesimals – are currently also present around the stars, and true planets may accompany these planetesimals. It is for this reason that the debris disks are true signposts of extrasolar planetary systems. Our understanding of the systems is reviewed by Backman and Paresce (1993).

Most of these debris systems have such low surface brightnesses that cooled telescopes in space are required for their study. Since IRAS, progress has been slow in studying all but the brightest systems. New planetary debris systems will be found most efficiently through far infrared photometry, at wavelengths where the contrast of the excess emission to the output of the primary star is relatively large. ISO should add to the discoveries of IRAS. However, the ISO mission may provide little opportunity to follow up on these latter discoveries in detail.

Spectroscopic investigation of the debris disks can allow identification of their composition and a comparison with material in our own solar system. Suggestive, but not conclusive, evidence of an olivine-like mineralogy has been found in the spectra of Beta Pic and several comets, which are remarkably similar (Knacke et al., 1993; cf. Figure 3.5); in part, the interpretation is

handicapped by the limited S/N and wavelength coverage available to ground-based observation. Extending these intriguing comparisons will require additional spectroscopic investigations of candidate debris disks discovered by IRAS, ISO, and SIRTf itself, but also additional reference spectra of comets orbiting the Sun. As is the case for debris disks, many such comets – particularly in the outer solar system – will have low infrared surface brightness and are best from space with a cooled telescope such as SIRTf.

3.2.3 The Outer Solar System

Predictions of a class of small objects in the outer solar system are confirmed by the recent discovery of a family of bodies known as the Kuiper Belt Planetesimals (Luu and Jewitt, 1996). The objects discovered by ground-based searches are approximately 200 km in diameter. The discoveries to date suggest that some 2×10^4 objects this size exist in a belt extending up to 18 degrees from the ecliptic. More recent results from HST (Cochran et al, 1995) have suggested that these large bodies are accompanied by a much larger number of planetesimals of ~10 km diameter, similar in size to the nucleus of Halley's Comet, but these HST results have yet to be confirmed.

The Kuiper Belt Planetesimals suggest the presence in the outer regions of our solar system of a debris disk of the type seen around other solar-type stars. The similarity between the sun's Kuiper Belt and the extra-solar debris disks has been underscored by calculations of the dust particle abundance and distribution in the Kuiper Belt (Backman, Das Gupta, and Stencel 1995). These results show that the distribution of dust within the Solar System – including both the Kuiper Belt material and the warmer zodiacal cloud interior to Jupiter's orbit – is very similar morphologically to that inferred from the IRAS observations for the dust distributions around Vega and Beta Pictoris; however, the amount of dust in the solar system is estimated to be as little as 10^{-4} of that associated with these stars.

3.3 Measurements Required from SIRTf

3.3.1 Protoplanetary Disks

SIRTf must be capable of carrying out the following measurement programs to discover and study protoplanetary disks:

Program 3.1 - Imaging surveys of nearby star formation regions.

Program 3.2 - Photometric study of selected targets to obtain spectral energy distributions and determine source geometry.

Program 3.3 - Composition studies through low resolution spectroscopy

Program 3.4 - Unbiased spectral imaging of stellar cluster cores.

Program 3.5- Detection of important volatiles by moderate resolution spectroscopy.

Program 3.1 - Imaging survey of nearby star formation regions.

A complete census of protoplanetary disks in a number of star forming regions is needed to address the issues of disk lifetime, the mechanism of disk dissipation, and the mass distribution of disks. Figure 3.1 depicts the spectral energy distribution at three stages in the life of a protostar, based on the models of Adams et al (1987). Although observations at all infrared wavelengths will be required, Figure 3.1 shows that, particularly in the earliest stages of star formation, the peak energy can best be observed in the far infrared (20–180 μm). When combined with groundbased measurements at 1 to 15 μm , these data will allow systematic surveys of regions of recent star formation to identify all members to a homogeneous (and low) level of luminosity – far below the luminosity of the sun – and also to provide data diagnostic of the presence of protoplanetary disks.

An example is provided by the well studied nearby star forming region in NGC 2264 (Lada, Young, and Greene 1993). SIRTf must have the sensitivity to detect the infrared emission from circumstellar dust shells and dust disks associated with even the lowest mass stars in this and other nearby clusters. Many of these young stars will still be ringed by systems of matter that are the initial step toward a planetary system. These systems are most readily seen in the mid-to-far infrared where their contrast with the stellar photosphere is greatest; thus the mid (15–30 μm) and far infrared data are essential for determining the frequency and luminosity function of potential disks in the cluster.

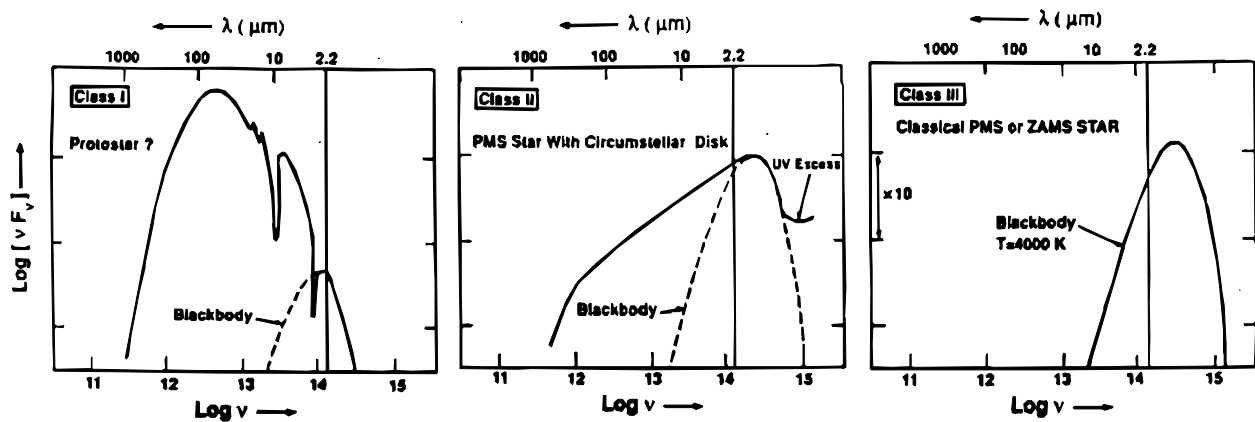


Figure 3.1 - The predicted evolution of the spectral energy distribution of young stellar objects, following a deeply embedded protostar through a stage where the circumstellar disk is prominent to the arrival of the star on the main sequence where it will spend most of its life. The models and classification are based on the work of Adams et al (1987).

The power of these surveys can be extended by surveying star clusters of different ages to understand the rate at which circumstellar material clears. For example, SIRTf should be able to make rapid surveys of clusters such as the Pleiades, Praesepe, and Hyades to detect the incidence of far infrared excess emission. These clusters must have been born under the same conditions in which stars are currently forming in the solar neighborhood. By selecting clusters of various ages and comparing with young star forming regions, we can measure the incidence of circumstellar disks as a function of age from ~1 million to ~1 billion years. With high resolution imaging and

spectroscopy from the ground to determine the incidence of binary systems in these clusters, we will also be able to determine the influence of companion stars on disk evolution.

As is shown in Figure 3.2, these imaging surveys should cover areas up to many square degrees to include a sample of up to ~ 100 sources in an individual star-forming cloud or cluster. It is desirable to adopt a strategy where the results are complete to some limiting luminosity, regardless of the emergent spectrum of the sources. This goal is suggested by the fact that various degrees of absorption and thermal re-emission by dust can shift the output spectrum of similar objects into widely differing wavebands. We therefore anticipate maps to homogeneous limits in λS_λ , which imposes a uniform luminosity limit of objects at the same distance. The bottom of the main sequence is $\sim 0.001 L_\odot$ and regions of star formation within 500 pc must be mapped at least to this limit. Several of the nearest star-forming clouds and clusters – between 100 and 500pc from Earth – which span a range in cluster age should be surveyed to allow a study of the time evolution of protoplanetary disks.

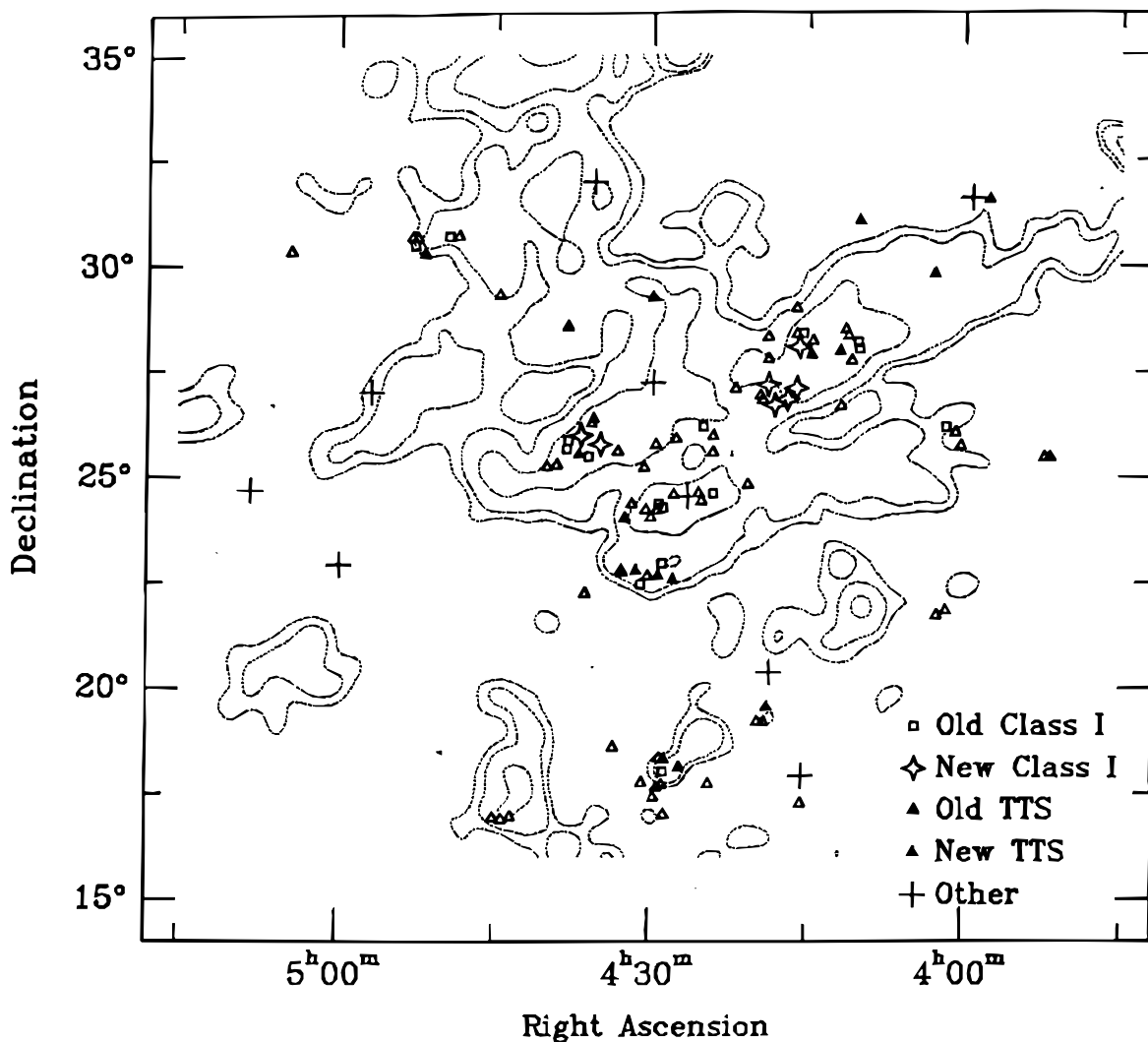


Figure 3.2 - A map of the dense molecular gas in the Taurus dark cloud with showing embedded young stars identified by IRAS (Kenyon et al, 1990).

These imaging surveys can be used to define complete samples of sources with a range of properties. SIRTf must be able to carry out the following types of follow-on investigations of this sample:

Program 3.2 - Photometric study of selected targets to obtain spectral energy distributions and source geometry;

Because most young stars likely to have protoplanetary disks are at distances too large to permit the disks to be readily resolved spatially, detailed photometry and comparison with models is the best available tool for understanding their structure. A recent example of this type of study is the modeling of the disks around young, massive stars by Hillenbrand et al (1992), as shown in Figure 3.3. This particular figure shows how the circumstellar emission varies with the inner radius of the disk. The observed infrared emission from a disk will depend on a range of properties: stellar luminosity, dust density, composition and distribution, and even the angle from which we view the disk. Some of these properties, in turn, will depend on the evolutionary state

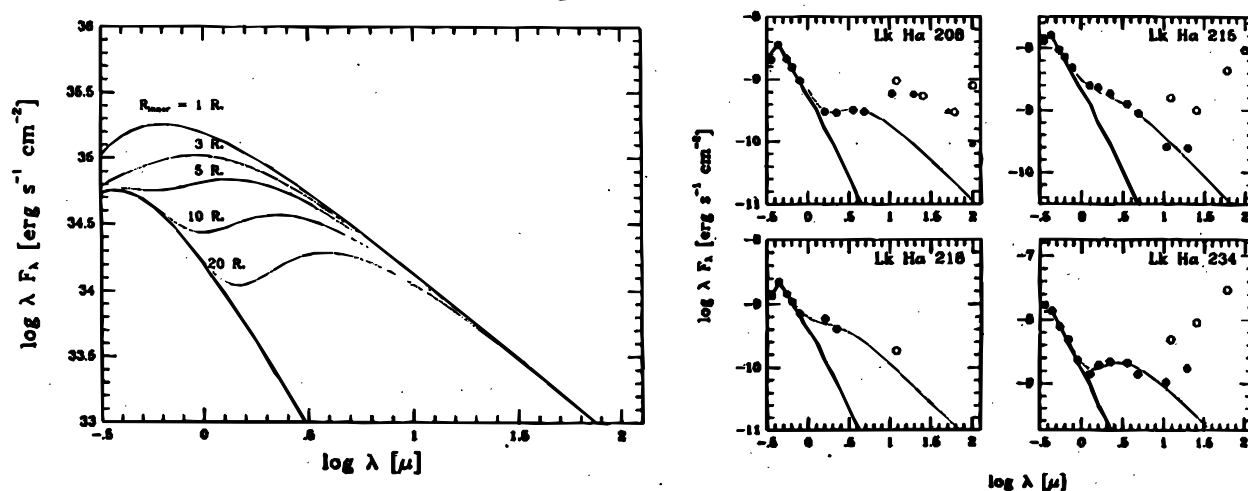


Figure 3.3 - Protostellar disk models from Hillenbrand et al (1992) are compared with existing infrared measurements on the right. The models show the predicted spectral energy distribution for a range of inner disk radii.

of the disk. Thus to test models of this type in detail, SIRTf needs to be able to provide low resolution spectroscopy over most of the 5 to 100 μm range to determine the spectral energy distributions of a sample of ~ 100 sources drawn from the above survey.

Program 3.3 - Composition studies through low resolution spectroscopy;

Spectra of protoplanetary and planetary debris disks can reveal the composition of the particles, including the presence and amounts of raw materials for the formation of life such as H_2O and organics. There is a wealth of relevant mineralogical features in the mid infrared. Since most of the protoplanetary disks will be unresolvable spatially by SIRTf, these features will have to be detected against the continuum of the central star [or, in absorption, if the orientation is favorable] and hence mineralogy will be possible only for relatively dramatic disk systems. The ice features at 62 μm is well removed from the peak of the stellar emission and may be more widely

detectable (Figure 3.4). In addition, ice and its mixtures with various volatiles may be identified by absorption in the 11.8 μm bands (Irvine and Pollack, 1968). The silicate features at 10 and 20 μm , discussed further below in the context of the planetary debris disks (Figure 3.5), will also be of

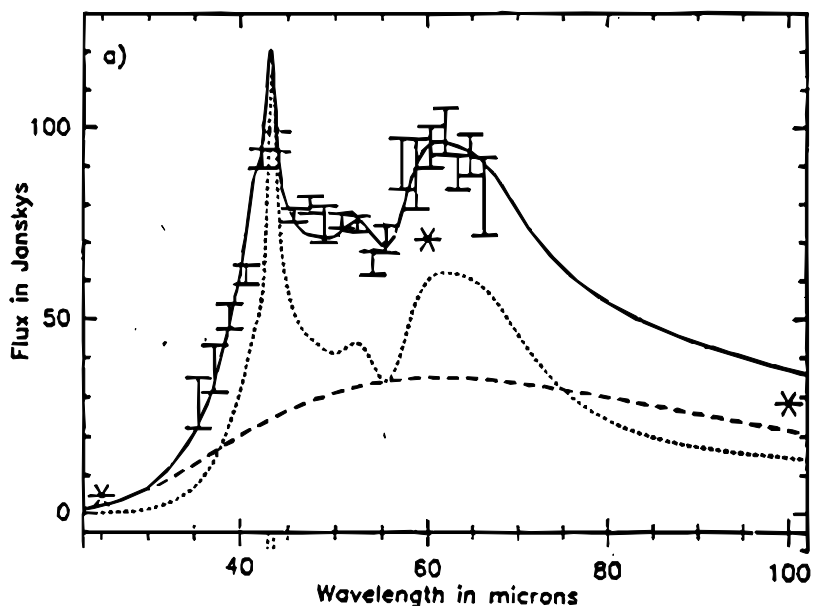


Figure 3.4 - Infrared spectrum of the “Frosty Leo Nebula”, (Omont et al; 1990), showing the emission features due to crystalline ice between 40 and 80 μm .

great interest in these systems.

Broad emission features at wavelengths between 5 and 11 μm have been detected in young stellar objects (Hanner et al, 1992) and in pre-main sequence stars (Schutte et al 1990) and attributed to Polycyclic Aromatic Hydrocarbons – moderately large, complex molecules. These emission features are also seen in the general interstellar medium, and their study in protostellar environments at low resolution $\{R \sim 20-50\}$ but high signal-to-noise can help to trace the physical and chemical pathways followed as interstellar material is transformed into new stars. These observations could be carried out on ~ 25 relatively bright objects from the sample identified in Program 3.1 and studied in Program 3.2 which appear on the basis of lower signal-to-noise spectral energy distributions to show interesting spectral characteristics.

Program 3.4 - Unbiased Spectral Imaging of Stellar Cluster Cores.

A complete picture of the content of an embedded cluster would require a complete set of spectral energy distributions. The density of embedded sources in the cores of some nearby clusters, such as NGC2264, can be exceedingly high (perhaps as high as 10/sq arc min), and the sources will be bright enough that low-resolution spectra – of every source down to the limiting sensitivity of the survey – can be obtained very quickly. In these cases, an observational strategy which obtains spectra at all spatial points would be an efficient approach to classifying the stellar content, determining the spectral energy distributions, and obtaining important chemical and physical information about the presence and properties of disks. The resulting “data cube” would simultaneously locate and provide a spectrum of every embedded star in the region, without the

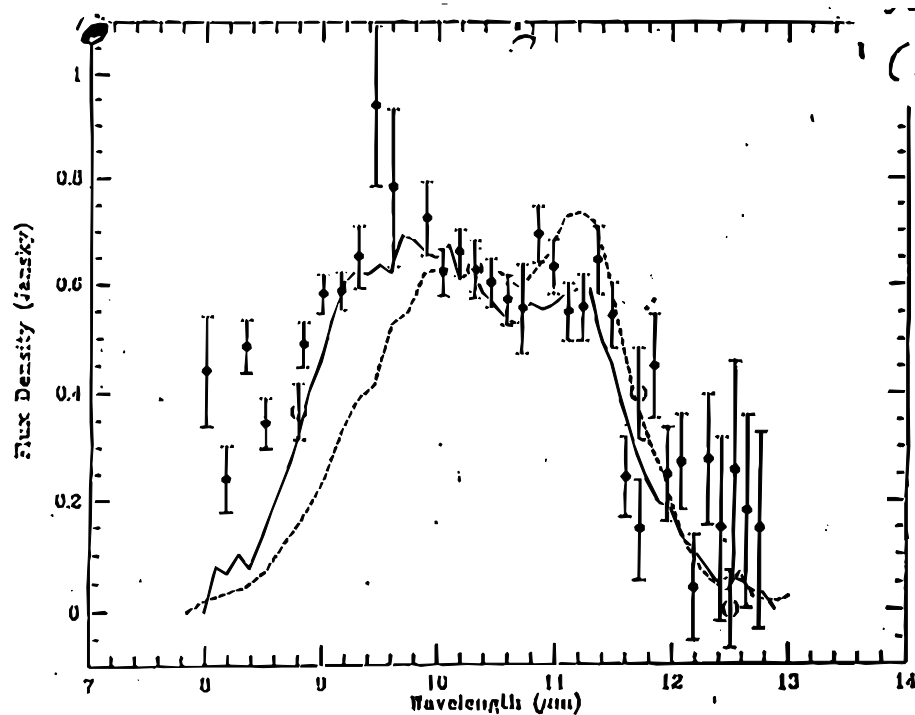


Figure 3.5 - 8-13 μm spectrum of the debris disk around Beta Pictoris (data points) showing an emission feature attributed to silicate minerals and a comparison to the spectra of comets in our solar system (solid and dashed curves). These data are taken from Knacke et al (1993).

selection bias imposed by selecting spectroscopic targets from an imaging survey. In addition, spectra obtained serendipitously of the regions between the sources will provide information about the chemical and physical properties of the regions of the cloud where stars have not yet formed. Comprehensive studies of this type of the central regions of selected clusters will nicely complement the more efficient, larger scale, purely imaging surveys described under 3.1 above.

As shown in Figure 3.3, wavelengths $\sim 5\text{--}30\ \mu\text{m}$ are well-suited to rapid identification of disks, and observations in this band can also determine the organic and mineralogical character of the circumstellar dust. If SIRTf achieves its low-resolution spectroscopic sensitivity goals over this spectral range, it would be possible to use an efficient spectral scanning mode to produce the spectral images. A scan rate of $\sim 0.1\ \text{arcsec/sec}$ and a slit width of a few arcsec would allow the sensitivity requirements established in program 3.1 to be reached. With spectrograph slits $\sim 1\ \text{arcmin}$ in length, this combination of parameters would allow the central $\sim 5 \times 5\ \text{arcmin}$ of a region such as NGC 2264 to be spectrally imaged in this mode in a reasonably short time.

Program 3.5 - Detection of important volatiles by moderate resolution spectroscopy;

Molecular and atomic lines should be observable in a variety of systems and will probe the composition and dynamics of the gaseous component of protoplanetary disks. The detection of water vapor absorption lines in T Tau stars in the near-IR (Shiba et al., 1993) shows the value of spectroscopy of volatiles in protoplanetary disks around young stars. Moderate spectral resolution ($R \sim 500 - 1000$) can be very useful, particularly in wavelength ranges where ground-based work is difficult or impossible even with 10-m apertures, often because these very same volatiles,

including the important water molecule H_2O , are components of the Earth's atmosphere. The aim is to study the "atmosphere" of the dusty disk, the gas overlying the midplane of the disk.

Theoretical models of H_2O line strengths have been computed by Neufeld and Melnick (1987) and Neufeld and Hollenbach (1994). They predict that water will be the primary coolant after H_2 in gentle shocks. Figure 3.6 shows the predicted intensity of these emission lines. The combination of spectrometers with large format, high performance arrays and operation in space away from terrestrial absorptions will give SIRTf an immense advantage in detecting H_2O in circumstellar and interstellar environments, provided that lines as weak as $5 \times 10^{-18} \text{ W/m}^2$ can be detected. This threshold allows the exploration of sources with one-tenth the line intensity predicted for the Orion region (Figure 3.6), which is expected to be the brightest object of this type. Similar arguments apply to studies of CO_2 and other volatiles, particularly for molecules that are highly abundant in the terrestrial atmosphere. SIRTf must also be able to detect the pure rotational transitions of H_2 at 17 and 28 μm . These observations – which are exploratory in nature – will be carried out on five of the brightest sources from each of the clouds studied in Program 3.1.

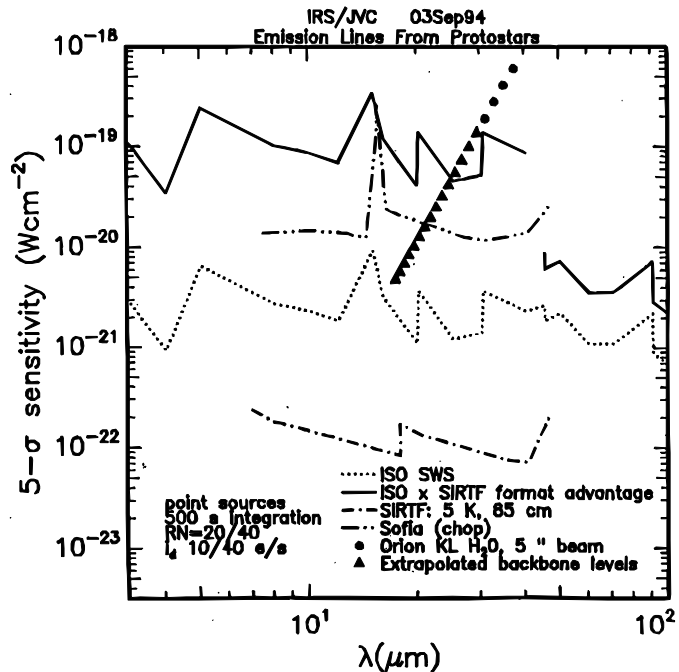


Figure 3.6 - Predicted line emission from highly excited H_2O molecules in the Orion molecular cloud, compared with the required spectrographic sensitivity of SIRTf.

3.3.2 Planetary Debris Disks

The study of planetary debris disks from SIRTf should include the following elements:

Program 3.6 - Searches for disks associated with samples of main sequence stars and around the nearest solar-type stars

Program 3.7 - High resolution imaging to resolve disk structures

Program 3.8 - Spectrophotometric studies to constrain disk models and composition

Program 3.6 - Searches for disks associated with samples of main sequence stars and around the nearest solar-type stars

Planetary debris systems can be found most efficiently through far infrared photometry, at wavelengths where the contrast of the excess emission to the output of the primary star is relatively large. Figure 3.7 depicts the energy distributions of debris disks spanning the known

range of dust densities, and compares these with SIRTf's sensitivity targets for imaging and low resolution spectrophotometry. The figure shows that if SIRTf achieves the predicted sensitivity levels, it will push the detection threshold for planetary debris disks down to the dust content of our solar system and will allow detailed studies of these systems and of the ones discovered by IRAS and ISO. Depending on the completeness of the work with ISO, SIRTf surveys of a more diverse stellar population may also be justified. In addition, the low resolution spectrometers on SIRTf can provide a unique capability to study the mineralogy of these systems and to detect water in them.

As shown in Figure 3.7, the median 100 μm excess emission from circumstellar dust around a G star is expected to be equal to the stellar flux at that wavelength (Aumann and Good, 1990). This emission arises at a distance of 50 to 200 AU from the central star, similar to the scale of the Kuiper Belt comet and debris disk around our own Solar System. Table 3.1 shows there are 9 stars between G0V and K0V within 6.8 pc, 4 of which are single. Many more candidates will lie between 6.8 and 20 pc. SIRTf must achieve sensitivities of ~ 2 mJy @ 70 μm and 10 mJy @ 160 μm to detect these excesses to a distance of about 20 pc, which permits sampling a significant number of stars. This same sensitivity level allows SIRTf to detect prominent disks such as that around Beta Pictoris to a distance as great as ~ 1 kpc, encompassing a large enough volume that disks can be sought around stars of unusual, transitional type.

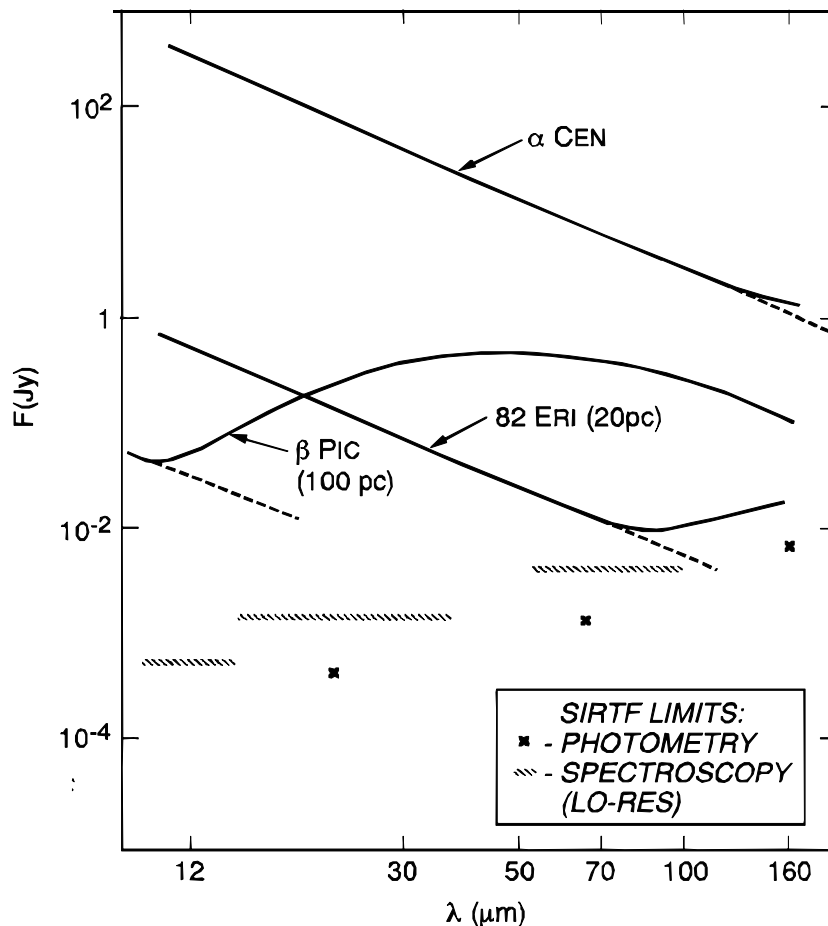


Figure 3.7 - Infrared spectral energy distributions of stars with planetary debris disks. The straight lines are the stellar photosphere, while the disk emission appears as an excess at long wavelengths. The three cases shown are: a) A solar-type disk around Alpha Centauri; b) A typical G-star disk around 82 Eri as it would appear at a distance of 20 pc; c) The well-studied disk around Beta Pictoris as it would appear at a distance of 100 pc. The SIRTf sensitivity targets for photometry and low-resolution spectroscopy (5σ in 500 s) are also shown.

Table 3.1 Candidate stars with possible Kuiper belt objects

Name	HD	BS	type	L/L_{\odot}	pc
α Cen A	128620	5459	G2 V	1.56	1.35
η Cas A	4614	219	G0 V	1.24	5.88
δ Pav	190248	7665	G8 V	1.07	5.71
82 Eri	20794	1008	G5 V	0.65	6.21
χ Boo A	131156	5544	G8 V	0.52	6.76
DM+02 3482 A	165341	6752	K0 V	0.46	5.13
α Cen B	128621	5460	K0 V	0.45	1.35
τ Cet	10700	509	G8 V	0.44	3.61
σ Dra	185144	7462	K0 V	0.37	5.68

At wavelengths shortward of 30 μm , SIRTf can search for warmer dust analogous to the inner zodiacal cloud within our own solar system. A single photometric measurement in this spectral band with noise $\sim 1\text{mJy}$ would establish the photospheric brightness level for comparison with the longer wavelength measurements or, in exceptional cases like Beta Pictoris, signal the presence of a large amount of warm material. Because of the great importance of the debris disk program,

SIRTf's initial search could encompass as many as 1000 nearby stars, chosen to represent a range of stellar types and characteristics.

Program 3.7 - High resolution imaging to resolve disk structures

Although modeling of the spectral energy distributions can provide information about the structures of these systems, it is susceptible to errors because of wavelength dependent emissivity effects in the constituent particles. These effects can appear either as spectroscopic features – silicates, PAHs, or ice – which could be detected as described below, or as smooth variations that would escape detection spectroscopically. In the latter case, the models can still be tested by imaging the systems to see if the size as a function of wavelength is successfully predicted by the model. Thus, although only relatively nearby debris disks can be imaged by SIRTf, these measurements will be of great importance in establishing “ground truth” for the validation of the models which will be used to determine disk structure and geometry from the spectral energy distributions which will be available for many systems. Similarly, we now have evidence that our own Solar System has a debris disk morphologically similar to those found by IRAS around stars like Beta Pic and Vega, in which a relatively dense and cool Kuiper Belt system rings a warmer but more tenuous inner zodiacal system. The amount of dust inferred in the solar system is 0.0001 of that in the prominent disks found by IRAS. Nevertheless, the capability to image dust systems around other stars as tenuous as that in our own solar system is very important scientifically, as it would bridge the gap and allow us to bring the full breadth of our understanding of the solar system to the interpretation of the extra-solar observations.

The predicted effective diameter for a system of gray particles goes as the square of the wavelength, whereas the diameter of the diffraction limited beam goes linearly with the wavelength, so imaging becomes easier at the longer wavelengths for such a system, if there is a radially continuous dust distribution. In agreement with this prediction, general efforts to image disks from the ground at 10 μm have been unsuccessful (e.g., Lagage and Pantin, 1994). However, grains of submicron size will have emissivities proportional to the inverse or inverse square of the wavelength, with an average value over this range substantially less than 1. Beta Pic is a good example. If one assumes large grains, the disk radius at 20 μm would be about 0.2", while in fact several observers (Telesco et al., 1988; Lagage and Pantin, 1994) have seen a disk more than ten times bigger! One has to assume a mean IR emissivity of 2% to get 150°K dust at

over 50 AU from this star. Since such small grains should have a limited lifetime against removal by the Poynting-Robertson effect, we are witnessing either the final stages of clearing of a young disk or the consequence of a relatively recent collision between two planetesimals. Similar issues are posed by the size of the Vega system (van der Blik, Prusti, & Waters 1994).

A number of other IRAS-selected stars are virtually certain to have resolvable disks at 70 μm . The Vega system is estimated to be 35" in diameter at this wavelength (van der Blik et al. 1994). Alpha PsA should have a disk of similar diameter, based on fitting its colors to estimated temperatures and computing the appropriate distance from the central star for gray particles of that temperature. Because of its wavelength coverage, IRAS emphasized systems with disks peaking near 60 μm (or shorter). The most distant systems listed in Table 3.1 should have Kuiper Belt-like planetesimal systems with diameters of about 35" at 70 μm . To achieve about 5 resolution elements across the images requires a combination of telescope aperture and post-processing which achieves a final resolution of $\sim 7''$ at 70 μm . Any cooler particles in these systems would be readily resolved at longer wavelengths, as would other disk systems with cool particles.

Figure 3.8 illustrates what SIRTf must achieve in this area by showing simulated images for four representative cases: A dust distribution identical to that inferred for our own solar system but placed around the nearby solar-type stars alpha-Centauri A and Tau Ceti (Table 3.1); a "typical G-star disk", based on the work of Aumann and Good, as it would appear around the star 82 Eri (Table 3.1); and the Beta Pictoris disk discovered by IRAS. In each case, the emission from the debris disks is compared with the Airy disk – which is the diffracted image of the star itself which would also be recorded by SIRTf. These simulations assume an 85 cm aperture for SIRTf; if the aperture is smaller, the Airy disk gets larger in angle, making the disk emission difficult to discern.

Such measurements would make full use of SIRTf's sensitivity and, in addition, require stable, fully-sampled images at wavelengths of 20 μm and longward which can be analyzed by deconvolution or super-resolution techniques to gain the maximum possible information about the faint debris disk structures. SIRTf should be able to image the very prominent Beta Pictoris system at 24 μm , but a final resolution $< 2''$ will be required to study the structure in this object. To image the "typical" or "solar type" disks around the nearest stars will require both the full resolution of an ~ 85 cm aperture and a data set which supports removal of the stellar Airy disk at a level of one part in 10 to one part in 100. Similar images will generally be unachievable by ISO. Thus SIRTf must achieve the performance adopted in these simulations to provide our first opportunity to image far infrared excesses around nearby stars to determine if they are analogous to the Kuiper Belt.

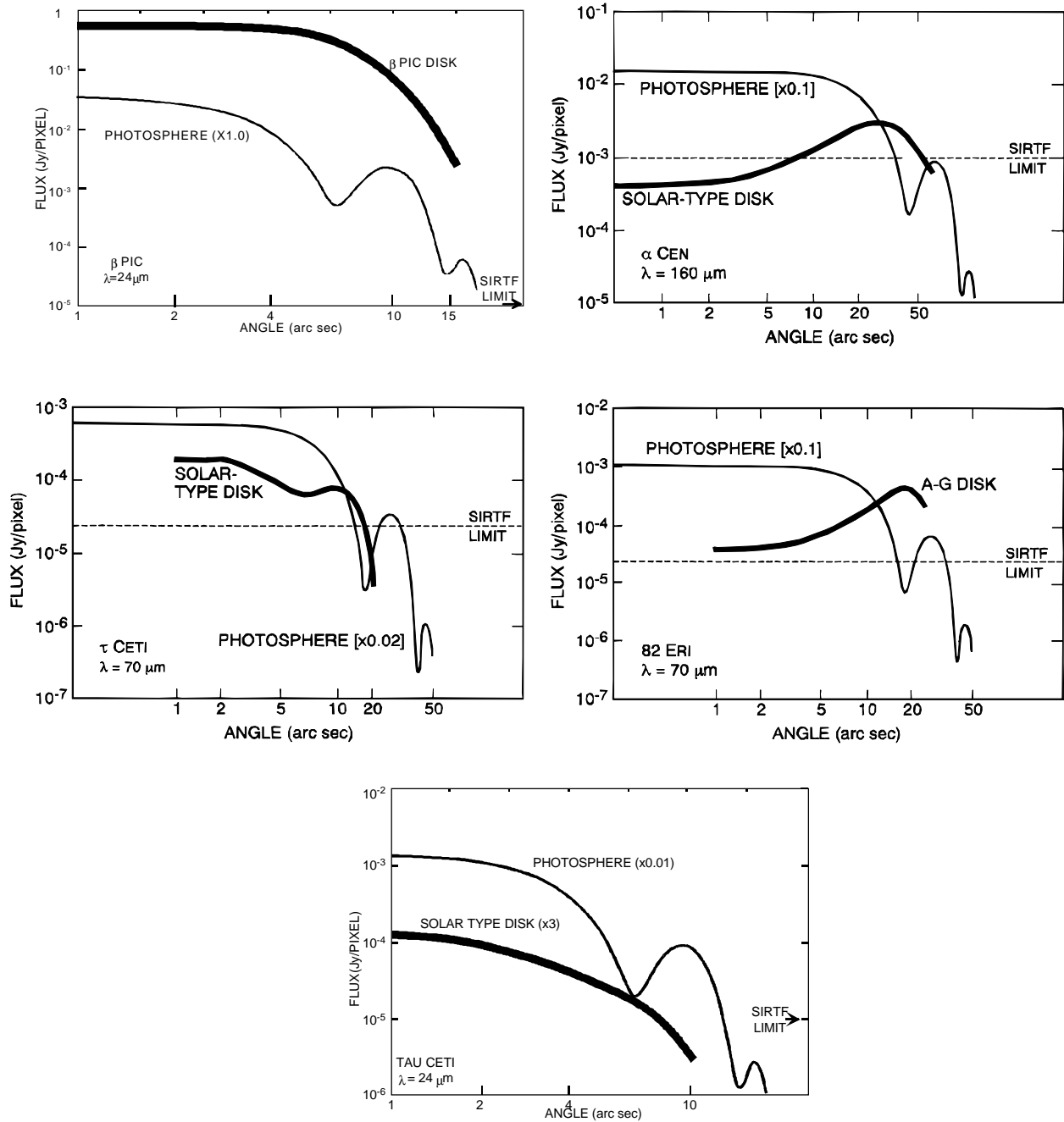


Figure 3.8 - Five simulations of measurements of planetary debris disks, as imaged by an 85cm SIRTf telescope with the sensitivity shown in Figure 3.7. The curves show flux per SIRTf pixel along the major axis of a disk with an inclination of 30 degrees to the line of sight, except that the known edge-on geometry of the Beta Pictoris disk is adopted. In each panel, the heavy line is the disk emission, and the lighter line “photosphere” the stellar Airy disk. Except for Beta Pictoris, the photospheric emission has been reduced by the factor shown in brackets, which indicates how well this contribution must be removed to produce the demonstrated contrast with the disk emission. The cases shown are: a) The Beta Pictoris disk @24 μm ; b) A solar-type disk around Alpha Centauri, imaged at 160 μm ; c) A solar-type disk around Tau Ceti, imaged at 70 μm ; d) A typical G-star disk (“A - G” disk) around 82 Eri; e) The solar-type disk around Tau Ceti, imaged at 24 μm .

Detection and imaging of the zodiacal emission (effective temperature of 280K) around nearby sunlike stars is a much more difficult goal than Kuiper belt-like debris disks. The decrease in the angular size of the thermally emitting region and the increase in stellar flux at shorter wavelengths counter the benefits of a smaller diffraction disk. However, if the Airy disk can be subtracted to the level of 1 part in 100 or better, it would be possible to image clouds just a few times denser than the solar system's zodiacal cloud at 24 μm around nearby stars such as Tau Ceti [cf. Figure 3.8e]; brighter zodiacal emission would be correspondingly easier to detect. For more distant systems, SIRTf's spectrometers, operating at sensitivity levels $<1\text{mJy}$ from $\lambda < 10 \mu\text{m}$ to $\lambda > 30 \mu\text{m}$, should also be capable of detecting the subtle systematic increase in flux above the stellar photosphere which would be indicative of small amounts of warm circumstellar material. This technique is probably applicable only to systems with at least an order of magnitude more zodiacal emission than is found in our solar system. In addition to their scientific importance and the significance of the links they would establish between our own solar system and the material around nearby stars, measurements in the 5-30 μm wavelength region would contribute to the planning for NASA's Origins program. This program has as an objective the operation of an infrared interferometer in the outer solar system, which would image nearby stars in the 12-20 μm region with the eventual aim of direct detection of planets around the stars. Direct or inferential estimates of the emission due to zodiacal-type dust clouds around such stars will be of great importance to the design and operation of this instrument.

Program 3.8 - Spectrophotometric studies to constrain disk models and composition

IRAS results suggest that debris disks may be found around up to 50% of main sequence stars, so SIRTf's photometric studies, building on the results from ISO and IRAS, should lead to the identification of many such systems around stars of all types. Studies of the composition of these many examples of solar-system type material will be of great interest. Silicate dust has a strong emissivity feature between 7 and 15 μm , and weaker emissivity features between 18 and $\sim 40 \mu\text{m}$; studies of small olivine grains (Mukai and Koike, 1990) suggest that there is little solid-state diagnostic information beyond 40 μm for these minerals. The spectra of Mukai and Koike (1990) and the IR mineral spectrum

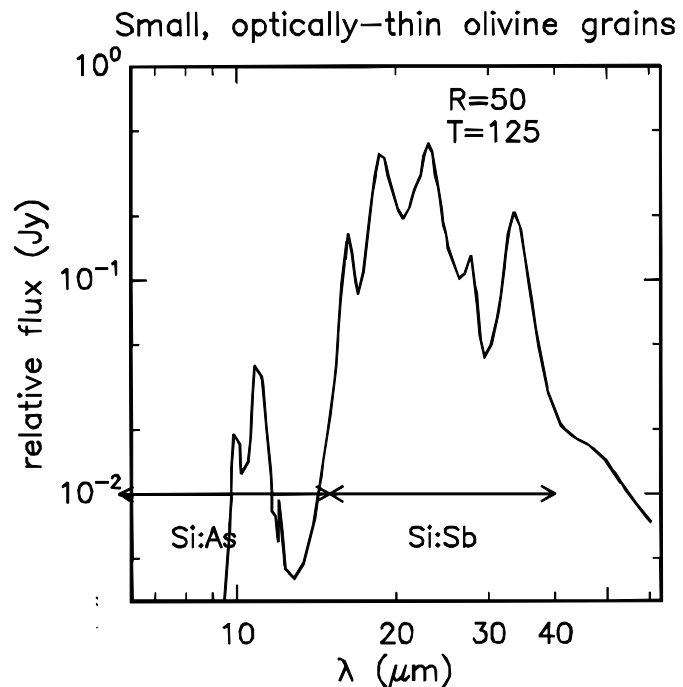


Figure 3.9 - Predicted spectrum of an optically thin disk of Comet Halley-like olivine dust at a temperature of 125°K, which is within the range expected for dust in both protoplanetary and planetary debris disks. The spectral range of SIRTf's two low-resolution spectrographs is also shown. The predicted spectrum is based on data from Mukai and Koike (1990).

atlas of Salisbury et al. (1992) show that a resolution (R) of 50 over the 7 - 40 μm range will be adequate to identify the mineralogy of silicate dust (Figure 3.9). Spectroscopic investigations of new planetary debris disks can be complemented by spectra of comets in our solar system, extending the comparison based to date only on two of the most prominent debris disk systems - Beta Pictoris and 51 Ophiuchus (Knacke et al, 1993, see Fig. 3.5).

Crystalline ice has been identified in the Frosty Leo object (Omont et al., 1990) with a sharp emission peak at 44 μm and a broad secondary maximum around 62 μm (Figure 3.4). Although ice has spectral features at shorter wavelengths (e.g., 3.1 and 11.8 μm), the temperature at which icy grains can survive is $< 100^\circ\text{K}$ and hence in optically thin systems such as debris disks these features would have to be detected by reflected light, where the contrast with the central star will be very low. Observations of the far infrared features are therefore the only viable means to detect ice in these systems.

As was the case for the protoplanetary disks, the infrared emission from a debris disk depends on a range of parameters - dust density, distribution, particle size - as well as on the particle composition. Thus many systems must be modelled in detail in order to separate important overall trends from the source-to-source variations in these parameters. SIRTf must observe at least 100 debris disk systems - some of which may be relatively faint examples identified in Program 3.5 - with high signal-to-noise in order to support this modeling.

3.3.3. The Outer Solar System

SIRTf's studies of the Outer Solar System and the Kuiper Belt have great scientific value and will also link SIRTf's studies of material around other stars to our vast body of knowledge of our own Solar System. These studies will include:

Program 3.9 - Spectrophotometric imaging of comets to determine their composition and heliocentric variability for comparison with studies of protoplanetary and planetary debris disks.

Program 3.10 - Photometry of known Kuiper Belt objects to provide accurate albedo and size determinations

Program 3.11 - A limited area survey to search for a new class of very dark objects;

Program 3.9 - Spectrophotometric imaging of comets to determine their composition and heliocentric variability for comparison with studies of protoplanetary and planetary debris disks.

Studies of the composition of new comets as they enter the outer solar system, or of periodic comets as they return to the solar vicinity or complete their orbital cycles, allow us to sample the material from which they formed - far from the sun during the early history of the solar system. This material is liberated from the solid cometary nucleus by solar heating and can be observed in the infrared as it absorbs and re-radiates sunlight. The composition and mineralogy of this cometary dust holds clues as to the nature of this protoplanetary material, and comparison of its spectra with those of the material in planetary debris disks will be indicative of the range of conditions under which planetary formation has occurred. Of particular interest will be the

complex of silicate and PAH features between 5 and 15 μm , as these sample potentially important inorganic and organic phases of the cometary dust. In addition, detailed analysis of the infrared data and comparison with visible images can determine the particle size, and the albedo of the cometary particles, and variations of these quantities with position in the coma and tail of the comet will be indicative of the processing which the particles undergo as they expand outward from the nucleus.

Bright comets observed near the sun, such as Halley (Campins et al, 1987; Hanner et al; 1987) and Giacobini-Zinner (Hammel et al, 1987) have been imaged over spatial scales ~ 1 arcmin; these images reach limiting 10 μm surface brightnesses ~ 200 MJy/sr. However, the 10 μm brightness will decline very rapidly with heliocentric distance [perhaps as quickly as the third or 4th power], so a comet just a few au from the sun – or a less active comet than these – will be ~ 100 times fainter than these objects. Thus we require that SIRTf's spectral observations reach a limiting surface brightness, ~ 1 MJy/sr. Because of the potential rapid variation of the cometary emission due to outbursts, jets, or rotation of the nucleus, it is desirable that a complete data set be obtained as quickly as possible over a region at least 2×2 arcmin in extent. This could make use of a spectral imaging mode, in which spectra are recorded continuously as a long (~ 1 arcmin) slit is scanned across the source. SIRTf's operational system will have to respond to new comets discovered in the outer system and introduce them into the observing schedule in as short a period as one day after the observation is approved. To track comets approaching perihelion within ~ 1 au of the sun, SIRTf will require non-sidereal tracking rates as high as 0.1 arcsec/sec.

Program 3.10 - Photometry of known Kuiper Belt objects to provide accurate albedo and size determinations

Large bodies several kilometers in size present insufficient surface area to give the observed infrared excesses of such stars as alpha Lyr, alpha PsA, and beta Pic. Dust particles are required, and they are likely to be produced in the required numbers only through collisions of larger bodies. The quantity of dust debris resulting from collisions depends critically on the resulting distribution of fragment sizes. Backman, Das Gupta and Stencel (1995) have prepared a detailed model of the Kuiper Belt dust which forms the basis of the "solar-type" dust disk discussed in the previous section. Thus, the population and dynamics of Kuiper Belts around main sequence stars may be directly related to debris disks to be imaged by SIRTf or to be inferred from infrared excesses. It is important to improve our knowledge of the planetesimals surrounding the sun to complement the exploration of the dust debris disks around other evolved stars.

Weissmann (1995), and Luu and Jewett (1996) tabulated the properties of dozens of large Kuiper Belt planetesimals, and we can anticipate that many more will have been discovered by the time SIRTf launches. SIRTf can easily detect the thermal emission of these ~ 100 km-sized Kuiper belt planetesimals, thus measuring their albedos and helping to determine their compositions. A 100-km radius object at Neptune's orbit (30 au from the sun) would have a flux of 3 mJy at 70 μm ; the required sensitivity of 0.25 mJy (5σ) allows the detection of objects as small as 15 km and as distant as 50 au. The observing strategy should make use of the fact that these are (slowly) moving targets. By suitably calibrating and then subtracting images obtained ~ 1 day apart, it will be possible to remove the fixed pattern confusion noise and enhance the visibility of the Kuiper Belt objects.

Program 3.11 - A limited area survey to search for a new class of very dark objects;

A SIRTf survey of the Kuiper Belt could identify objects of very low albedo which were not detected at visual wavelengths. The visual wavelength results allow us to predict that the surface density of objects with $r \sim 100$ km is approximately 4–5 per square degree, and smaller objects appear to be more abundant. SIRTf's survey would be of greatest import if it were sensitive to a new population which was about as abundant as the visibly detected objects and thus provided a comparable amount of mass. This implies that SIRTf be able to survey about ~ 0.2 sq degree of the ecliptic plane to a flux level of 0.25 mJy @ 70 μm , in order to discover objects as small as ~ 15 km; the deep survey could be accompanied by a larger area, shallow survey, covering ~ 1 sq degree to ~ 2.5 mJy (5σ) looking for larger targets. Each survey must be carried out twice to detect the motion of the Kuiper Belt planetesimals and must be accompanied by a shorter wavelength survey to eliminate "foreground" asteroids.

Table 3.2 Science Requirements for the Protoplanetary and Planetary Debris Disks Program

Program	Wavelength Range (μm)	Sensitivity Required	Spectral Resolution $\delta\lambda/\lambda$	Spatial Resolution arcsec	# of Targets	Comments
3.1 - PPD Census	6.5 - 180	0.6,0.7,2,6,15mJy@ 6.5,8,24, 70,160 μm - all 5 σ -	0.25	7x($\lambda/30 \mu\text{m}$) to minimize confusion with background	5 sq degree in each of five clouds	survey to .001 L_{\odot} luminosity @500 pc
3.2 - PPD Spectral Energy Distribution	5 - 40, 50 - 100	0.6 mJy, (5 - 15 μm) 2 mJy (15 - 40 μm) 6 mJy (50 - 100 μm)- all 5 σ	~0.05	Match slit size to resolution, sensitivity	~100 sources from above survey	support modelling of brighter sources
3.3 - PPD Dust Composition	5 - 40, 50 - 100	1 mJy (5 - 15 μm) 4 mJy (15 - 40 μm) 10 mJy (60 - 100 μm)	0.02 to 0.05	Same as above	~25 sources from survey 3.2	High s/n needed for mineralogical studies
3.4 - Unbiased Spectral Imaging of Cluster Cores	5 - 30	0.6,0.7,1.5,3 mJy, @ 6.5,8,16,30 μm , 5 σ per spatial, spectral resn' element	0.02	Same as above	5x5 sq arcmin in each of five clouds	Obtain spectra at all spatial points - use continuous scan if available
3.5 - Gas in PPD's	10 - 40	~5 $\times 10^{-18}$ w/m ² , 10 σ per spectral res element	0.001 to .002	same as above	~ 25 sources from survey 3.1	Look for H ₂ O and other volatiles
3.6 - Debris Disk Search & Photometry	24 - 160	1 mJy, 10 σ at 24 μm ; 2 mJy, 10 σ at,70 μm ;10 mJy, 10 σ @160 μm	0.25	7x($\lambda/30 \mu\text{m}$) to minimize confusion with background	~1000 selected targets in survey mode	Study debris disks as distant as 1 kpc
3.7- Debris Disk High Resolution Imaging	24 - 160	~100 KJy/sr, 5 σ per pixel @ 24,70,160 μm	0.25	2"@24 μm ; 7"@70 μm , 16"@160 μm , including gains from super-resolution	~20 nearby stars, ~20 stars from IRAS, ISO, SIRTF surveys	Use super-resolution @ 24,70,160 μm to resolve central voids, etc. Subtract Airy disk to ~1%.
3.8- Debris Disk Composition and Structure	5 - 40, 50 - 100	1 mJy, 5 - 40 μm 5 mJy, 50 - 100 μm 5 σ per spectral resolution	~0.02 to 0.05	Match slit size to resolution, sensitivity	~100 targets from IRAS, ISO, SIRTF surveys	Supports modelling and determines composition

		element				
3.9 - Spectral imaging of comets	5 - >15	1MJy/sr, 1 σ , per spatial, spectral resn element	~0.02	Same as above	Map up to 25 sq arc min in ~5 comets; get spectrum at each spatial point	Follow comet through orbit; need track rates up to 0.1 arcsec/sec
3.10- Kuiper Belt Object Photometry	70	0.25 mJy @ 70 μ m, 5 σ	~0.25	20"	~50 objects from optical surveys - as small as ~15km	albedo, size determination; moving targets
3.11 Kuiper Belt Survey/Search for Dark Objects	70	0.25 mJy @ 70 μ m, 5 σ	~0.25	20"	search 0.2 sq. degree, repeat to detect moving targets	Also survey ~1 sq degree to ~2.5mJy, 5 σ , to find larger objects

4 Ultraluminous Galaxies and Active Galactic Nuclei

4.1 Impact on Science

Understanding Active Galactic Nuclei (AGN) has been a major thrust of modern astrophysics for three decades. AGN—quasars, radio galaxies, and Seyfert galaxies—have compact, luminous nuclei that contain highly excited gas that exhibits high velocity motions. It is generally thought that AGN are powered by the gravitational energy released as matter accretes onto massive blackholes. It has been known since the early 1970's that many AGN emit the bulk of their luminosity at infrared wavelengths. IRAS showed that far-infrared-selected galaxies are the dominant population of extragalactic sources for $L > 5 \times 10^{11} L_{\odot}$ in the local ($z < 0.1$) universe, more numerous than quasars in the same luminosity range [Figure 4.1]². The most luminous of these infrared-selected systems have been discovered at redshifts up to 2.3. For comparison, a large galaxy like our own Milky Way has a luminosity $\sim 10^{10} L_{\odot}$.

The similarity in luminosities and a variety of other observations suggest an evolutionary link between far-infrared-selected galaxies and optically selected quasars. This hypothesis can be tested by infrared spectroscopic observations that measure ratios of lines of differing excitation energy emitted near the nucleus. As shown in Figure 4.2, such ratios can be used to distinguish between thermal and non-thermal ionizing sources. This picture is supported by the first spectroscopic results reported from ISO (Lutz et al, 1996).

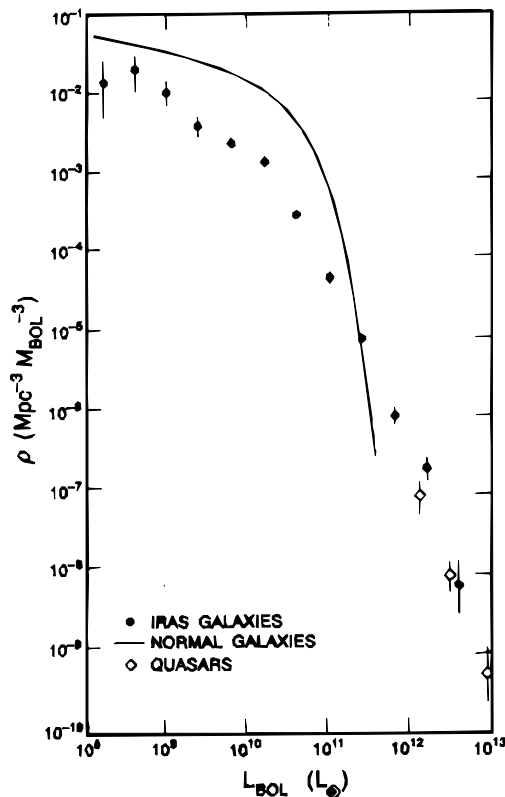


Figure 4.1 - Local luminosity distribution of Extragalactic Objects. The space density vs. bolometric luminosity for infrared galaxies ("IRAS galaxies"), normal galaxies and quasars in the local Universe. The vertical bars indicate statistical uncertainty. The plot shows that infrared-luminous galaxies are the dominant population of extragalactic sources for $L > 5 \times 10^{11} L_{\odot}$.

² The redshift (z), defined as the fractional increase in observed wavelength, $(1+z) = \text{observed wavelength/emitted wavelength}$, is related to the recession velocity (v) of the source and the speed of light (c) by the formula $(1+z) = \sqrt{\{(1+(v/c))/[1-(v/c)]\}}$. In standard cosmological models it is also true that $(1+z) = R(\text{now})/R(\text{then})$, where $R(\text{now})/R(\text{then})$ is the ratio of the scale of the Universe at the current epoch, when the photon is received, to the scale at the epoch when it was emitted. Thus when we observe a galaxy at $z=3$ we look back to an epoch when the Universe was 25% of its current size; the corresponding age depends on cosmological parameters as shown in Figure 5.2.

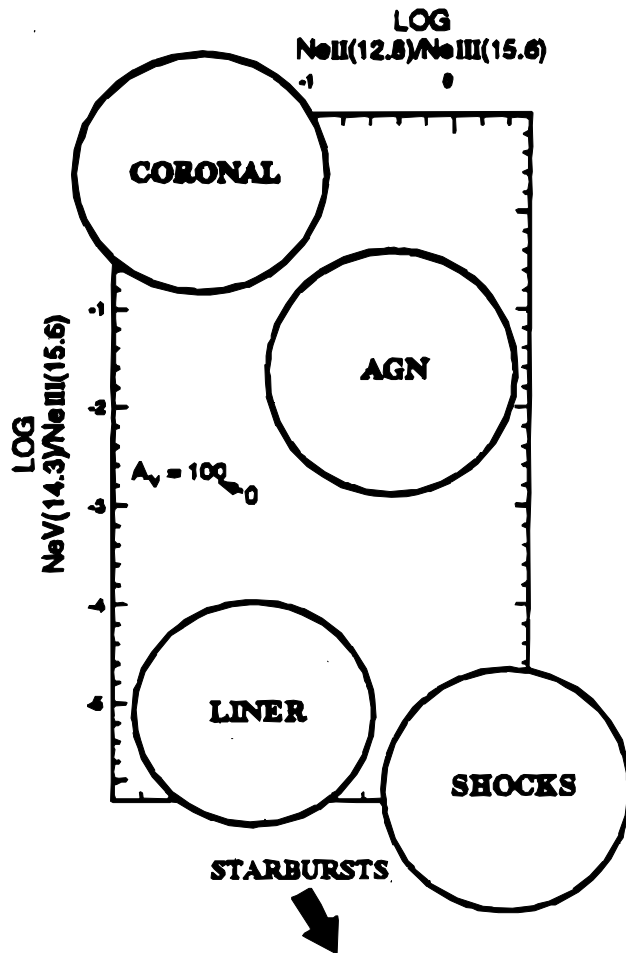


Figure 4.2 - Spectroscopic Diagnostics in the Infrared. Measurements of three emission lines of ionized neon in the 12–15 μ m region allow a source to be placed on this line-ratio diagram and the processes that excite the plasma in the source to be determined. The circled regions show the area of the diagram where sources of different types are predicted to lie (Voit, 1992).

The arrow labeled A_v indicates that this technique is insensitive to the amount of overlying dust and can be used to probe the deeply embedded luminosity sources that power ultraluminous infrared galaxies.

By observing infrared luminous galaxies over 90% or more of the age of the Universe, SIRTf should have unprecedented capability to study the properties and evolution of this population, the relationship between these galaxies and AGN discovered by other techniques (e.g. X-ray-selected AGN from AXAF deep surveys), and the relationship of AGN to the evolution of galaxies in general. SIRTf's goals in this area are: 1) To undertake deep, multi-wavelength surveys that will provide large numbers of objects for detailed study as well as for statistical analyses of the evolution of infrared-bright galaxies; 2) To measure spectroscopic redshifts, and hence to determine distances and luminosities, of the most extreme systems discovered in SIRTf imaging surveys and in surveys from prior missions, including IRAS, ISO, WIRE, HST, and AXAF; 3) To probe spectroscopically the interior regions of these dust-enshrouded galactic nuclei, to determine the nature of the excitation of these systems and their underlying power sources and to determine whether these characteristics evolve with cosmic time; 4) To detect these objects at high enough redshifts ($z > 3$) to explore not only the character of the infrared luminous galaxies but also the early history of the Universe.

4.2 Previous Investigations

By achieving the above-stated goals, SIRTf will make unique contribution to the study of central science questions that are raised by these luminous galaxies. These questions include:

4.2.1 What is The Link Between Ultraluminous Infrared Galaxies and Quasars?

An Ultraluminous Infrared Galaxy (hereafter a ULIRG) is a galaxy with an 8–1000 μ m luminosity greater than $5 \times 10^{11} L_{\odot}$. The most luminous known ULIRGs, FSC10214+4724

(Eisenhardt et al 1996) and FSC15307+3253 (Cutri et al 1994), have $L \sim 2 \times 10^{13} L_{\odot}$. IRAS studies have shown that the vast majority of ULIRGs are found in merging and interacting systems. Some ULIRGs show spectral evidence of high gas velocities similar to those seen in quasars and Seyfert 1 galaxies. Most show no direct evidence for an associated classical AGN; however, it has been suggested (e.g., Sanders et al. 1987) that there is a direct evolutionary sequence between ULIRGs and quasars.

The basic idea [Figure 4.3] is that two gas-rich galaxies collide and eventually merge via the dynamic friction of the gravitational encounter. During the merging, the gas, which loses angular momentum much more easily than the stars via dissipative processes such as cloud-cloud collisions, falls rapidly to the center of the combined system. During this phase, the infrared luminosity of the system may be powered by bursts of star formation as the compressed gas undergoes gravitational collapse.

If a massive black hole exists or forms in the center of the merged galaxy, as seems to be common (Kormendy et al, 1996), it can accrete the nearby high density material at a high rate. Such an accreting black hole could have the luminosity and other characteristics of a quasar, but the surrounding cloud of gas and dust effectively shrouds it and absorbs the primary radiation produced in the accretion process. The absorbed energy is re-emitted in the infrared, and the system is observed as a ULIRG. Eventually the accretion-driven luminosity disrupts the surrounding cloud, revealing the underlying quasar. The overall shapes of the uv-optical-infrared energy distributions of galaxies and quasars with $L > 5 \times 10^{11} L_{\odot}$ can be ordered in a sequence which is highly suggestive of this evolution [Figure 4.4].



Figure 4.3 - Cartoon of an embedded, emerging QSO. A collision between two gas rich galaxies [top] could cause interstellar material to accrete onto a black hole in the nucleus of one of the galaxies [middle], creating a quasar which would be observed initially in the far infrared but, with time, would blow away the enveloping dust and appear at visible wavelengths.

Recent imaging of nearby quasars by HST (Bahcall, Kirhakos and Schneider, 1995) has shown several systems that are suggestive of this picture. The appealing thing about this picture is that it links the most luminous objects in the universe, the quasars, with normal galaxies like the Milky Way; however, the fundamental ideas here must be tested carefully.

4.2.2 At What Redshift Do Heavy Elements Form?

The most distant known ULIRG, FSC10214+4724, has a redshift of $z=2.286$, corresponding to a lookback time of $\sim 10^{10}$ years (see figure 5.2). FSC10214+4724 has recently been shown to be gravitationally lensed (see, e.g., Eisenhardt, et al. 1996). Taking into account a lensing magnification of ~ 25 at infrared wavelengths, the intrinsic luminosity of the source is $2 \times 10^{13} L_{\odot}$. FSC+10214 shows that ULIRGs exist at large lookback times and thus at an early epoch in the life of the universe. IRAS was able to detect this distant object only because of the lensing magnification. SIRTf must be able to detect unlensed objects of this luminosity at even larger redshifts.

Despite its cosmic youth, FSC10214+4724 appears to have a heavy element abundance consistent with solar abundances, i.e., heavy elements constitute about 1% of the total mass. Although higher redshift quasars

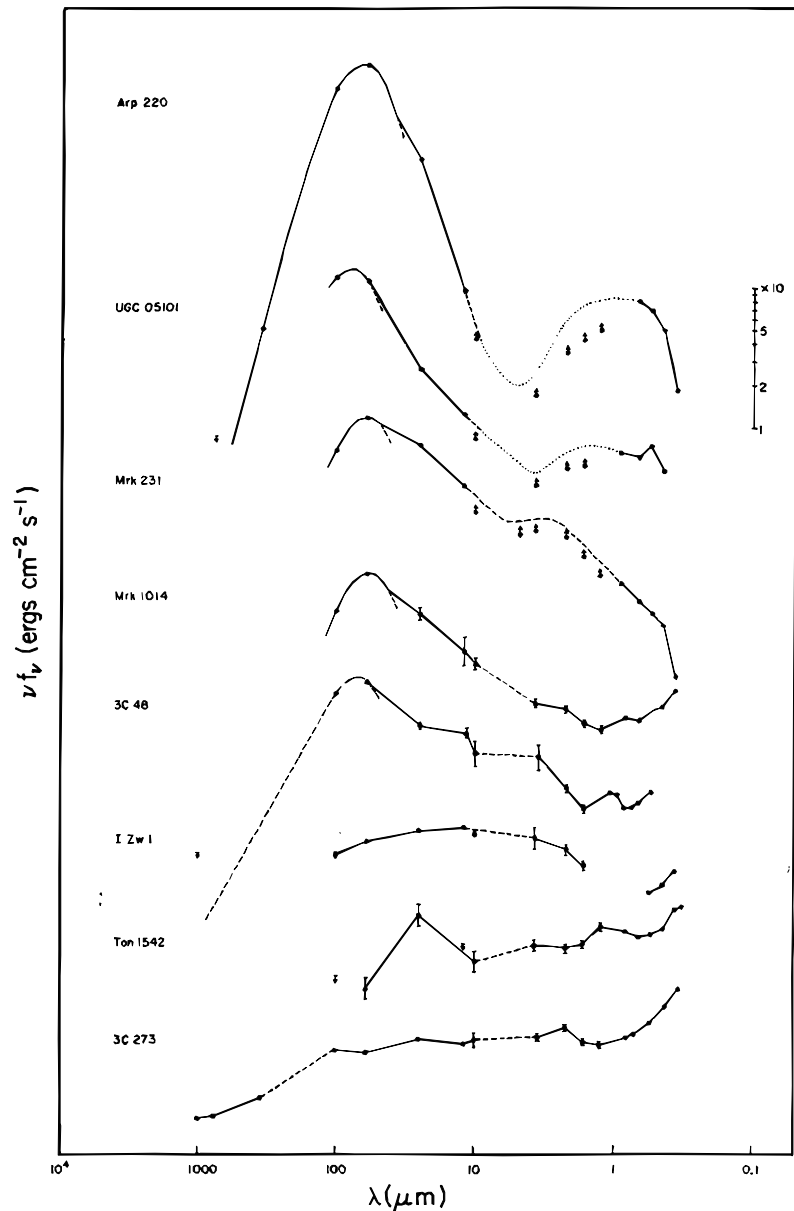


Figure 4.4 - Spectral energy distributions of objects of comparable luminosity [$\sim 1 \times 10^{12} L_{\odot}$] but with a continuous range of physical characteristics. The principal luminosity sources in Arp220 [top] are shrouded by dust so that most of the observed power is radiated in the far infrared. At the other end of the scale, 3C273 is a classical quasar. This sequence illustrates the evolution suggested by Figure 4.3. Dashed lines are interpolations over wavelengths where no measurements are available, while dotted lines indicate an upward correction to measurements which sampled only a portion of the galaxy (Sanders et al, 1987).

are known from emission line spectroscopy to have heavy elements, the abundance of heavy elements in FSC10214 is far larger than in the other, more distant systems. A cutoff redshift in the detection of infrared bright galaxies – such as might be revealed by a deep survey – would indicate a qualitative change in composition of these systems and thus the redshift at which heavy elements are formed in the early universe. The reason for this is that dust which radiates the infrared radiation from the ULIRGs is composed of heavy elements, so that the onset of the ULIRG phenomenon could signal the first appearance of substantial quantities of these elements.

4.2.3 What Are The Implications Of The Ultraluminous Galaxies For Galaxy Formation?

A 1% heavy element abundance can only be achieved by processing a substantial fraction of the primordial hydrogen/helium mixture through stars. Thus the observation of a metal-rich galaxy at $z=2.286$ already constrains the formation epoch of the galaxies, and detection of higher redshift systems with similar heavy element abundance would place even tighter limits on the galaxy formation process.

4.3 Measurements Required from SIRTf

In order to make substantial gains in our understanding of the ultraluminous infrared galaxies and their place in the universe, SIRTf must be able to:

A. Search for ULIRGs at $z > 5$. The presence of such systems, and the implication that stellar processes would have proceeded for a substantial prior period, would imply that the epoch of galaxy formation occurred at a redshift that is incompatible with current ideas of the formation of large scale structure in the universe.

B. Test the evolutionary picture linking infrared galaxies and quasars by determining the luminosity function of the infrared galaxies as a function of redshift, thereby directly determining whether the infrared-luminous systems share the strong cosmological evolution of quasars.

C. Probe dust enshrouded nuclei with IR spectroscopy to establish excitation, ionizing source, and heavy element abundance as a function of redshift.

A SIRTf program to study ultraluminous infrared galaxies should contain the following elements:

Program 4.1: Establish a data base of $\sim 10^5$ extragalactic sources to a flux limit of ~ 1 mJy at $70 \mu\text{m}$, which will contain candidate ULIRGs to $z > 5$

Program 4.2: A complete redshift survey for all objects with $f_{\nu}(70 \mu\text{m}) > 10$ mJy found in Program 4.1.

Program 4.3: Spectroscopic follow-up of faint objects found in Program 4.1 with the highest ratio of $L_{70\mu\text{m}}/L_{\text{nearIR-vis}}$

Program 4.4: A spectroscopic survey to investigate excitation conditions and energy sources in ULIRGs.

Program 4.5: Spectroscopic follow-up of sources from the WIRE deep survey.

Program 4.6: Photometric follow-up of sources from the WIRE deep survey.

Program 4.1 - Establish a data base of $\sim 10^5$ extragalactic sources to a flux limit of ~ 1 mJy at $70 \mu\text{m}$,

A $70 \mu\text{m}$ flux of 1 mJy is about 200 times fainter than the IRAS limit and far fainter than the faintest ISO sources. Thus we do not know how large an area of sky would have to be surveyed to establish this sample. Estimates range from 5 to 50 square degrees, and we should bear in mind that a determination of the density of sources on the sky at low flux levels would be an important early outcome of the survey. Thus the survey strategy might have to be modified following initiation of the observations. The sample size is chosen to create a database which contains significant numbers of the ULIRGs, which constitute about 3% of the sources in the flux-limited IRAS survey. Wavelengths for the survey are $70 \mu\text{m}$, $24 \mu\text{m}$, and $160 \mu\text{m}$. This survey should overlap the HST deep surveys, the AXAF deep fields, the Sloan Digital Sky Survey, and the VLA deep survey. Sources as luminous as FSC+10214+4724 and FSC15307+3252 would have a $70 \mu\text{m}$ flux ~ 3 mJy at $z=7$ and will be detected readily if they exist at such an early epoch (Figure 4.5). Sources five times less luminous would be detectable at $z > 5$, and the survey sensitivity is established on this basis so that it can reach below the tip of the luminosity function. With a $70 \mu\text{m}$ flux density limit of 1 mJy, a system with the $70 \mu\text{m}$ luminosity of Arp 220, (the closest and best studied example of the ULIRGs), would be detected to $z \sim 2$, as is shown in Figure 4.5. Thus this survey can detect objects familiar in the local Universe to cosmological distances. Figure 4.5 also demonstrates that carrying out the survey at several

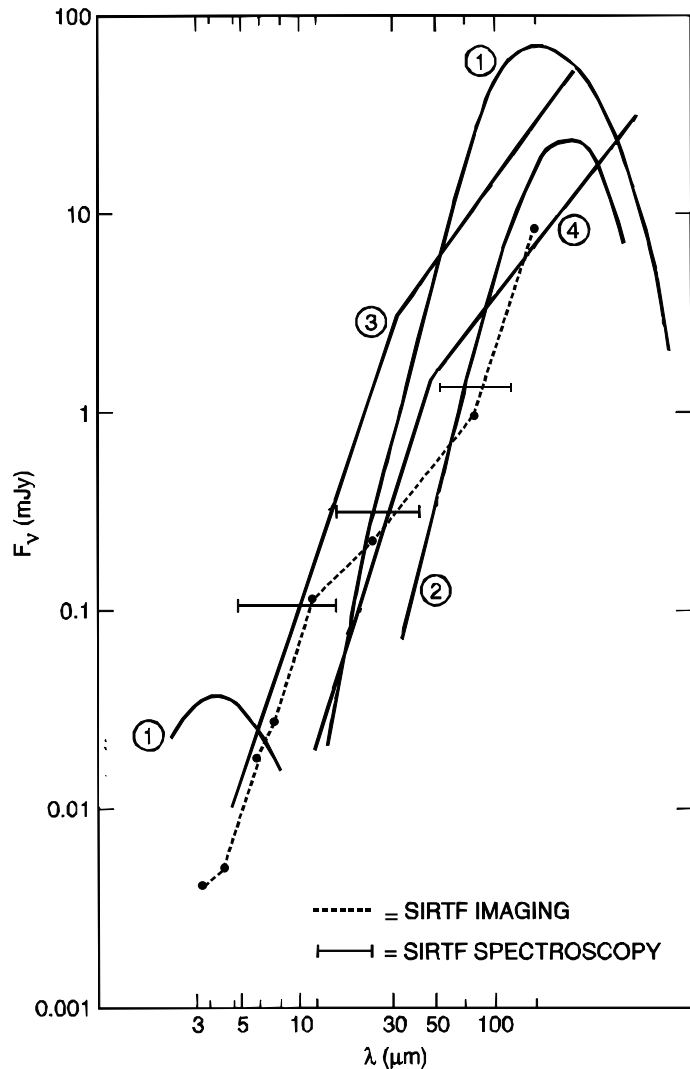


Figure 4.5 - Flux vs redshift for Arp 220 and FSC 15307. Arp220 is shown as it would appear at $z=1$ [] and $z=2$ [], while for FSC 15307 the adopted redshifts are $z=4$ [] and $z=7$ []. An $\Omega=1$ cosmology is assumed. The SIRTf limits are shown for imaging [5σ in 500 sec] and for spectroscopy [5σ in 10000 sec].

wavelengths allows rapid selection of potentially interesting objects by virtue of the flux ratios among the various bands. A $70\mu\text{m}$ beam size of $25''$ or smaller is required so that confusion does not prevent SIRTf from achieving the required sensitivity.

In general, we expect many infrared-luminous galaxies to be members of interacting pairs, with typical separations $\sim 30\text{Kpc}$. In additional examples, a foreground or background galaxy will appear close to the ultraluminous object due to chance projection effects. It will be important in both cases to be able to locate the source of the infrared emission to facilitate follow-up observations, both from SIRTf and from the ground. Although the details depend somewhat on the cosmology adopted, the angular diameter corresponding to 30Kpc reaches a minimum of about $3''$ near $z\sim 1$, and is larger at both higher and lower redshift. This angle is a small fraction of the SIRTf beam at $70\mu\text{m}$, so that centroiding of the image center will be required to achieve this angular resolution. The signal/noise requirement of this program should be sufficient that such centroiding can be carried out on sources at least as faint as 5 mJy , which will permit accurate positional determinations for $\sim 10^4$ sources.

Program 4.2 - A complete redshift survey for all objects with $f_{\nu}(70\text{ mm}) > 10\text{ mJy}$ found in Program 4.1.

Spectroscopic redshifts must be measured for the brightest 3000 of the 10^5 sources. Scaling from the local universe, roughly 3% (100) of these sources will be ULIRGs. The most extreme of these systems will have visual R magnitudes fainter than $R = 23$. The goal is to have complete redshift information for all 3000 of these sources with adequate time left in the SIRTf mission to plan and carry out follow-up observations of the most interesting objects, in particular those that can be seen only with SIRTf. This “bright object” survey will identify all FSC 10214-like objects up to $z\sim 5$ and will be able to measure the luminosity function of sources 10 times more luminous than Arp 220 to $z= 1.5$. Approximately half the objects will be brighter than 19th magnitude, and so should be in the Sloan Digital Sky Survey redshift survey. Most of the rest of the work can be done on 4m class telescopes, with the faintest optical targets that can be done from the ground (i.e. $R\sim 24\text{mag}$) requiring the use of 8–10 m class telescopes. A handful of the sources might be expected to have no identifiable optical counterpart due to source confusion at the faintest optical magnitudes.

Roughly 50–100 of these sources – those with no optical counterpart or those with visible counterparts having $R > 24\text{ mag}$ – will require SIRTf spectrographic measurements using low resolution mode for redshift determinations. This will require spectra of sources with flux densities in the range $0.1\text{--}1\text{ mJy}$ in the wavelength range $5\text{--}40\mu\text{m}$. Redshift determination will rely on the strong infrared dust emission/absorption features that span the $3.3\mu\text{m}$ to $12\mu\text{m}$ wavelength range in the rest frame of the source. Spectral resolution of 50–100 is adequate for measurement of these broad features, and extending the measurements to $40\mu\text{m}$ allows redshifts >5 to be determined.

Program 4.3 - Spectroscopy of extremely red objects.

Comparisons of deep SIRTf surveys with the deepest fields surveyed by AXAF and HST (both WF/PC2 and NICMOS) will be extremely important. Objects that can be seen only in

infrared observations will hold vital clues to the early evolution of galaxies and AGNs. The most interesting sources for SIRTf will be those that *only SIRTf can see*. The Sloan survey will have imaging data to $R=23$ mag, so the basic criterion for inclusion in a sample of extremely red objects will be sources detected by SIRTf but NOT detected in the Sloan. This will provide a sample of sources with $L_{\text{IR}}/L_{\text{r}} > 50$, which therefore emit most of their energy in the infrared. Roughly 2% of the objects in the 1 mJy survey, or 2000 sources, should meet this criterion. It is assumed that ground based imaging of these red objects at $2 \mu\text{m}$ will provide flux densities, morphologies, and source identifications for some of these objects. This should be done early in the mission so that SIRTf follow-up observations can focus on objects not easily studied from the ground.

For these faint SIRTf sources, SIRTf itself must be capable of determining redshifts. SIRTf will selectively observe the ~ 100 most promising sources from this list, using the low resolution spectroscopic mode to determine the redshift. The redshift survey of the 1 mJy sample will permit the luminosity function of sources of the Arp 220 class to be determined to $z \sim 2$. Note that both this and program 4.2 may require that the positions of faint $70 \mu\text{m}$ infrared sources be determined with sufficiently small uncertainty from SIRTf's imaging observations to permit placing of these targets on the spectrograph slits. Alternatively, a peak-up mode for the spectrograph could be used to acquire the targets in real time by measuring their broadband fluxes.

The combination of programs 4.2 and 4.3 will lead to the derivation of the luminosity function of infrared luminous galaxies out to $z \sim 2$ for $L \sim 10^{12} L_{\odot}$, and appropriately larger redshifts for higher luminosity systems. This will permit direct comparison with the quasar luminosity function that has now been determined out to $z > \sim 4$, as well as identifying the prime targets for SIRTf follow-up observations, such as those described in 4.4 below. By using these very luminous objects as beacons to probe the early Universe, these programs could extend our knowledge of the presence and properties of galaxies in the Universe far beyond our current horizon, which is set by the QSO cutoff around $z \sim 5$.

Program 4.4 - Investigation of excitation conditions and energy sources in ULIRGs

Based on programs 4.2 and 4.3, sources will be selected for spectroscopic study to determine the excitation conditions in heavily dust enshrouded objects. The purpose of these observations is to establish the excitation conditions, luminosity sources and metal abundance as a function of lookback time. Spectral resolving power in the range $500 < R < 1000$ will be required to detect the narrow emission lines of these gas phase species. The prime targets are the suite of forbidden lines of various stages of neon accessible to SIRTf [Figure 4.2]. Prime lines are [NeV] $14.3 \mu\text{m}$ and [NeVI] $7.6 \mu\text{m}$ which can be observed in targets from $z \sim 2$ (NeV) to $z > 4$ (NeVI). Many other forbidden lines of abundant elements, such as lower ionization stages of neon, as well as magnesium, argon, and sulfur, can be observed as well. These lines will permit more detailed abundance and excitation analyses to be done, and should result in the assessment of the contribution of stellar photoionization and AGN photoionization for ULIRGs as a function of redshift. In addition, the use of all the neon lines from the full range of ionization stages from NeII to NeVI will permit the abundance of neon, and hence that of the heavy elements, to be determined relative to hydrogen as a function of redshift.

ISO can do the closest sources, i.e. $z < 0.1$, but SIRTf must reach $z=1$ to begin to explore evolutionary effects on cosmological time scales. To detect the neon lines in ultraluminous galaxies at great distances requires a five-sigma sensitivity to line emission of $\sim 3 \times 10^{-18}$ w/m²; this is the predicted intensity of the NeII 12.8 μ m line in Arp220 at $z \sim 1$. For extremely important sources, out to $z > 5$, SIRTf must be able to do these observations even though long integrations may be required. For closer objects, very high signal-to-noise-ratio measurements must be made to enable the detailed abundance and excitation studies called out above. These will require a sensitivity $\sim 1 \times 10^{-18}$ w/m². These measurements also require that the target be accurately placed and maintained on the spectrograph slit, so that a SIRTf line flux measurement can be quantitatively compared with those at other wavelengths and from other facilities. This requirement will drive the pointing (or offsetting) accuracy and stability for SIRTf. Overall, the SIRTf program would encompass 100 targets at a range of luminosity and redshift.

Program 4.5 - Spectroscopic follow-up of sources from WIRE.

SIRTf's explorations will frequently complement and extend those of other space and ground-based programs, including ISO, WIRE (scheduled for launch in 1998), AXAF (also to launch in 1998), and HST. SIRTf spectroscopy of extremely red objects, some of which will undoubtedly be found in the WIRE surveys, is addressed in Program 4.3. Nevertheless, sources from WIRE deserve special discussion, because the WIRE surveys will be by far the most sensitive mid-infrared surveys available when SIRTf flies.

WIRE's moderate depth survey will cover more than 100 square degrees of high latitude sky to 5-sigma levels of 1 mJy at 25 μ m and 0.3 mJy at 12 μ m, about a factor of 100 fainter than the faintest flux levels reached by IRAS. The intention of this survey is to determine the evolution of infrared luminous galaxies out to redshifts of greater than 1, to determine the contribution of star formation to the luminosity of the universe at $z=0.5$ and beyond, and to search for high luminosity systems to $z \sim 3.0$. The WIRE survey at 12 and 25 μ m will complement SIRTf's 70 μ m survey, although it will not probe as far back into space and time. SIRTf should conduct a redshift survey of the most intriguing targets identified in the WIRE mission. Their availability at the start of the SIRTf mission will allow an early start on spectroscopic investigation of infrared galaxies, as well as providing a means of learning the properties of targets at the flux density levels that WIRE can achieve.

There may well be many targets found by WIRE that will not be identifiable with optical counterparts, and SIRTf will be required to obtain spectra for these targets, which may amount to perhaps as many as 1% of the WIRE catalog of 10^5 sources, or 1000 objects in all. The most basic determination of the nature of these objects, as extragalactic or galactic, and their distance determination will require SIRTf's spectroscopic observations. It is likely that the most interesting individual objects discovered by any of these missions, i.e. those at the highest redshifts and perhaps new classes of sources, will be those without optical counterparts, and SIRTf observations will therefore be crucial to elucidating their nature.

In order to obtain such observations, SIRTf will have to be able to obtain low resolution spectra in the region 8–40 μ m of sources as faint as 0.3–1 mJy. The initial SIRTf program should sample 10% of the unidentified WIRE sources, or up to 100 objects. Note that the WIRE sources

will have positional uncertainties of $\sim 4''$, so either a positional determination from SIRTf or the use of a peak-up mode will be required to enable these observations.

Program 4.6 - Spectral Energy Distributions of WIRE Sources

The scientific strategy of WIRE uses the 12 to 25 μm flux ratio as an indicator of the luminosity of the galaxies found in its survey. This, combined with the number counts of galaxies at various flux levels, can be used to study the evolution of the starburst/infrared galaxy population. SIRTf measurements of a sample of WIRE galaxies across the infrared band can test the validity of this ratio as a luminosity indicator. Based on the WIRE faint survey limit of $\sim 0.4\text{mJy}$ at 25 μm , SIRTf's measurements must reach flux levels $\sim 10\ \mu\text{Jy}$ at 6 and 8 μm , 3 mJy at 70 μm , and 10 mJy at 160 μm . These objectives could easily be achieved by locating SIRTf's deep surveys in the near infrared and at 70 μm to coincide with deep fields measured by WIRE.

Table 4.1 Science Requirements for the Ultraluminous Galaxies and Active Galactic Nuclei Program

Program	Wavelength Range (μm)	Sensitivity Required	Spectral Resolution $\delta\lambda/\lambda$	Spatial Resolution arcsec	# of Targets	Comments
4.1 Definition of 70 μm selected sample	24-160 μm	1 mJy @ 70 μm (6σ) 250 μJy @ 24 μm (6σ) 9 mJy @ 160 μm (6σ)	0.25	~20" at 70 μm to minimize confusion	>5 square degrees Target is 100,000 sources @ 70 μm	Simultaneous observations @ 24, 70, 160 μm . Centroid 70 μm sources brighter than 5mJy to ~3"
4.2 Redshift survey of 70 μm objects brighter than 10 mJy	5-40 μm	0.1 mJy, 5-15 μm 0.3 mJy, 15-40 μm 5 σ per resolution element	~.02	Match slit size to resolution, sensitivity	100 targets	Get redshifts in IR for sources not measured at other wavelengths
4.3 Redshifts for selected sources with 70 μm flux 1mJy-10mJy	5-40 μm	0.1 mJy, 5-15 μm 0.3 mJy, 15-40 μm 5 σ per resolution element	~0.02	Match slit size to resolution, sensitivity	100 targets	Select faint targets from (4.1) with highest L(ir)/L(vis)
4.4 Excitation mechanisms in IR galaxies	10-40 μm	1-3x10 ⁻¹⁸ w/m ² (5 σ line sensitivity)	~0.001 to 0.002	Match slit size to resolution, sensitivity. Place and hold target accurately on slit.	100 targets from above surveys	Need ~2% absolute line flux determinations for abundance studies out to z~0.1
4.5 WIRE galaxy spectroscopy	5-40 μm	1 mJy@25 μm ; 0.3 mJy@12 μm (5 σ per res element)	0.02	Match slit size to resolution, sensitivity	100 targets from WIRE survey	Redshift determinations looking for hi-z objects. Need peak up or position determination from SIRTf as source position is uncertain.
4.6 WIRE galaxy photometry	3.5-160 μm	6,6,10,30 μJy @3.5,4.5,6,8 μm ; 0.3,1.5,10 mJy @24,70,160 μm , all 5 σ	0.25	2-3" @8 μm and below; 20" or better at 24, 70 μm	100 targets from WIRE deep survey	complete SED for characterization of sample to 0.1xArp220 @z=0.5

5 The Early Universe

5.1 Impact on Science

An outstanding challenge to modern astrophysics is to understand when and how galaxies like our own Milky Way formed. Today we see a range of galaxy types with a variety of morphologies, stellar populations, and star formation rates. Some galaxies have unusual phenomena in their centers while others are relatively quiescent. (The Milky Way, from our admittedly less than ideal vantage point, appears to be a fairly typical large spiral galaxy). Galaxies are organized into a hierarchy of structures defining the largest scale objects in the Universe. While we have many tantalizing clues about how the current state of the Universe has come to be, we are missing the most critical data from the earliest epochs of galaxy formation and evolution. SIRTf should be a powerful “time machine” to view the early Universe directly to discover the processes that we can only speculate about now.

SIRTf, rather than a telescope operating at shorter wavelengths, can play the role of time machine because of a fundamental property of the Universe – its expansion. This expansion carries more distant galaxies away from us at higher velocities than nearby objects, and these expansion velocities shift light from short to longer wavelengths – or blue to red – causing

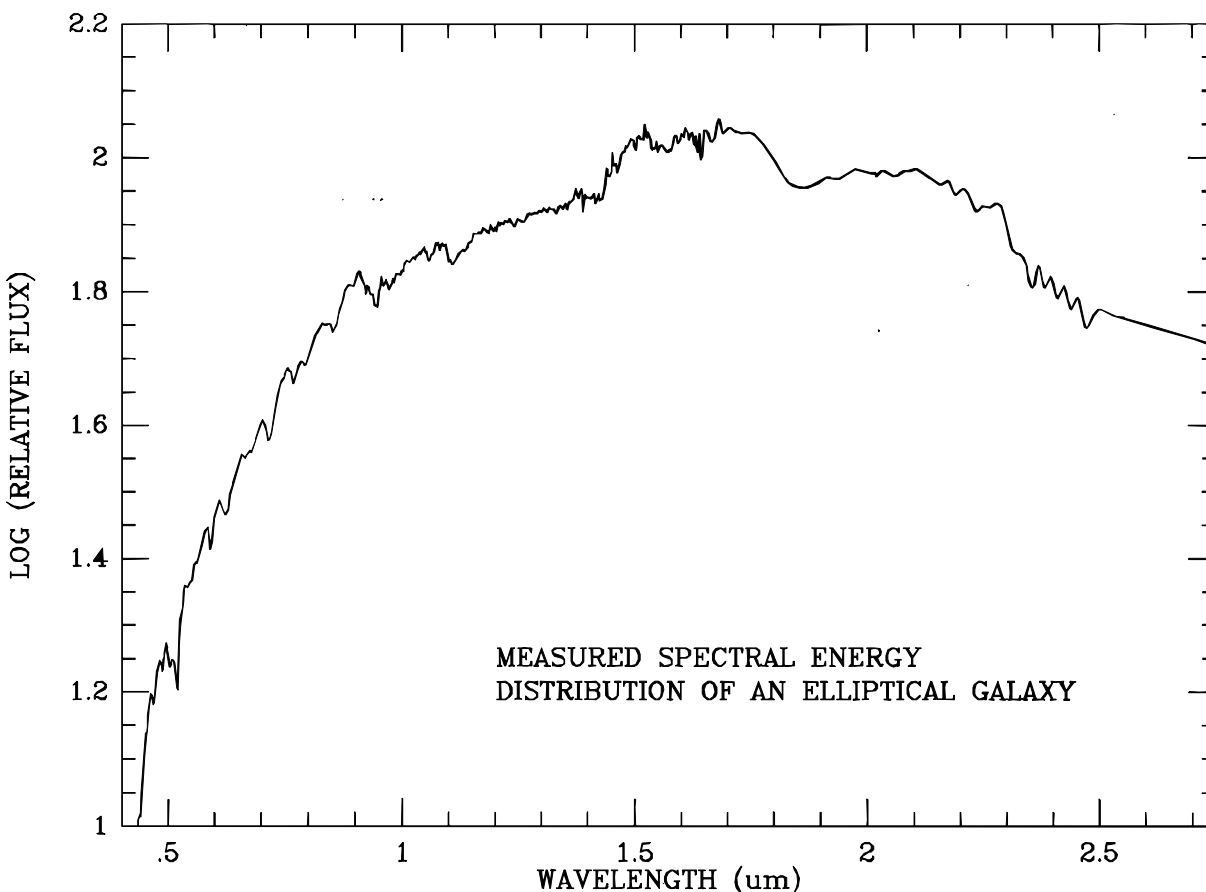


Figure 5.1. - Measured spectrum of a current-day elliptical galaxy (Rieke 1996), showing the 1.6 μm emission feature due to H- opacity and the 2.3 μm absorption feature due to CO.

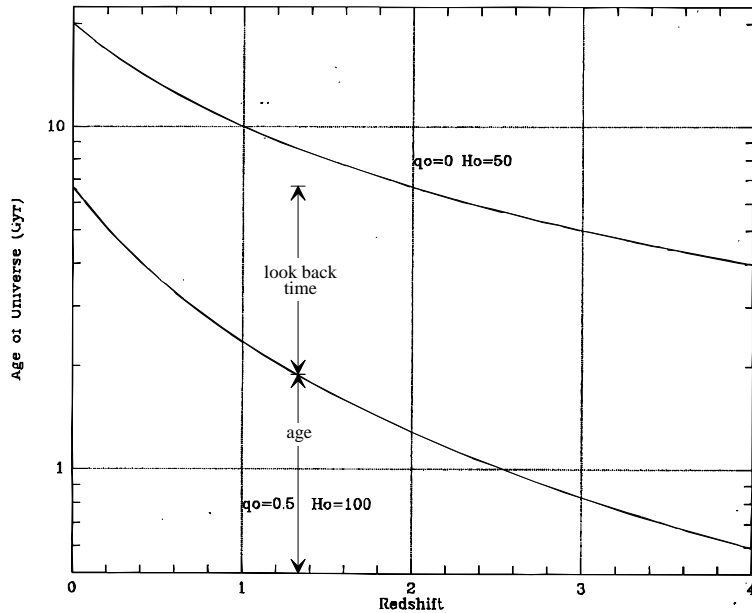


Figure 5.2. - The age of the universe vs. redshift for two possible choices spanning the range of common values for cosmological parameters. The lookback time for, e.g., redshift 1.35, is simply the difference between the age of the universe at redshift 0 and at redshift 1.35.

redshifts. For example, the energy output from stars in a galaxy has a peak at a wavelength of $1.6 \mu\text{m}$ and drops sharply at $2.3 \mu\text{m}$ (see Figure 5.1). By measuring the location of the peak and the drop, one can estimate the redshift of a galaxy and therefore its distance. Because of the time it takes light to travel to us, the more distant an object we can identify from its redshift, the younger the object we can study. Figure 5.2 shows the relationship between redshift, look back time, and the age of the Universe. Thus if SIRTf could observe the $1.6 \mu\text{m}$ peak redshifted to beyond $6.4 \mu\text{m}$, (i.e., at a redshift > 3) it would be studying a galaxy as it was when the Universe had less than a quarter of its current age and size.

Infrared observations sensitive enough to detect starlight from very distant galaxies are not possible beyond $2.5 \mu\text{m}$ from groundbased facilities because of thermal emission and low atmospheric transmission, or beyond $1.8 \mu\text{m}$ from HST due to high thermal emission. SIRTf must extend this wavelength range to $\sim 8 \mu\text{m}$ to produce a major increase in our ability to probe the early Universe. In addition, SIRTf should be able to study objects at intermediate redshifts to determine the contributions of the formation of new stars and the aging of the pre-existing population to the overall evolution of galaxies. Finally, SIRTf should probe a small area of sky with sufficient sensitivity to produce images in which the sky is essentially covered with galaxies. These “confusion-limited” images will contain as much information as SIRTf can obtain about the distribution of galaxies in time and space. They will also be of value in searching for a true extragalactic infrared background which might date from an epoch prior to that of galaxy formation.

To achieve these objectives requires that SIRTf meet the following measurement goals:

- 1) To survey the sky at near infrared wavelengths to detect several hundred normal galaxies at $z > 3$ and to determine the redshifts of these and of the many other galaxies which will be included in these images; 2) To survey the sky at far infrared wavelengths to study star formation in normal galaxies and how it varies with cosmic epoch; 3) To obtain confusion-limited images at several infrared wavelengths which will provide the most penetrating look at the extragalactic sky achievable with SIRTf.

5.2 Previous Investigations

5.2.1 Galaxy Evolution and Star Formation in Galaxies

Many different lines of evidence are being actively pursued to discover how galaxies formed and evolved. Observations of the most distant galaxies and quasars are filling in some of the gaps in our knowledge between the state of the Universe now and what it was after the Big Bang.

The most distant objects known in the Universe are quasars, which exist in the centers of some galaxies and are powered by accretion of gas onto massive black holes. Many questions about the relationship of

quasars to normal galaxies can be raised, such as what fraction of all galaxies harbor black holes in their nuclei, but past observations of quasars provide two significant clues about the state of the early Universe. First, spectra of quasars reveal that some elements too heavy to have formed in the Big Bang exist in even the most distant quasars. Heavy elements (or “metals”, which in the present astronomical context means any element beyond boron in the periodic table) are produced by nucleosynthesis in stars and in supernova explosions. Thus the existence of heavy elements in quasars, which have been observed to redshifts almost as great as 5, demonstrates that the first episodes of star formation occurred very early in the history of the Universe – at redshifts of 5 or greater. Second, the numbers of luminous quasars have not remained constant with time. Figure 5.3 shows that the relative number of luminous quasars increases rapidly from the present to a redshift of about 2 and is clearly declining beyond redshift 3. Does this change in the numbers of luminous quasars indicate a special epoch in the evolution of galaxies?

Another course that is being pursued to learn about the evolution of galaxies is simply discovering and counting them. Surveys executed at several different wavelengths can help us to understand whether an epoch of enhanced star formation occurred in the past and what the basic geometry of the Universe is. Because very large format infrared detectors are only now becoming available, such surveys have been conducted almost exclusively at visible wavelengths up until now. As is shown in Figure 5.4 (Glazebrook et al 1994) these surveys have revealed an unexpectedly large number of faint, blue galaxies. Detailed study of these galaxies shows surprisingly that they are located at rather modest redshifts of only 0.3–0.4, making them very puzzling objects but not probes of the early Universe. These surveys refer to light emitted

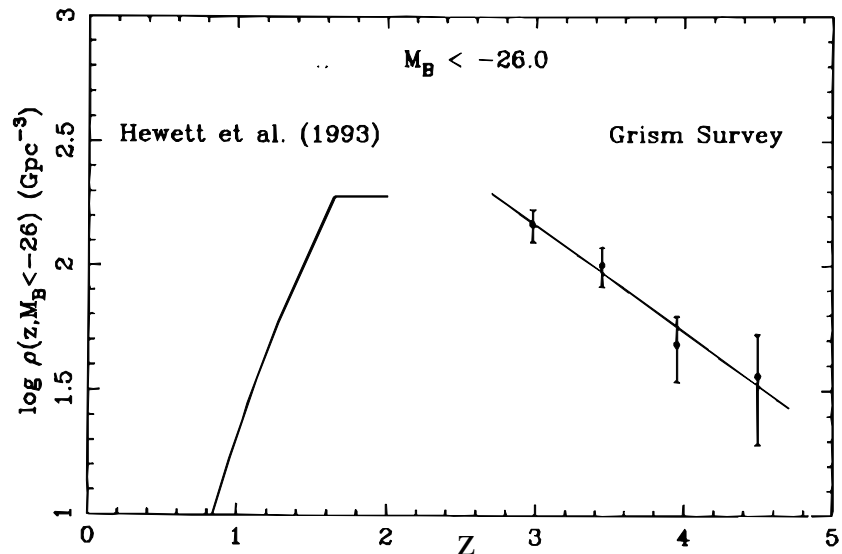


Figure 5.3 - Co-moving space density of $M_B < -26$ quasars as a function of redshift, z , from Schmidt, Schneider, and Gunn (1995). The figure assumes $q_0=0.5$

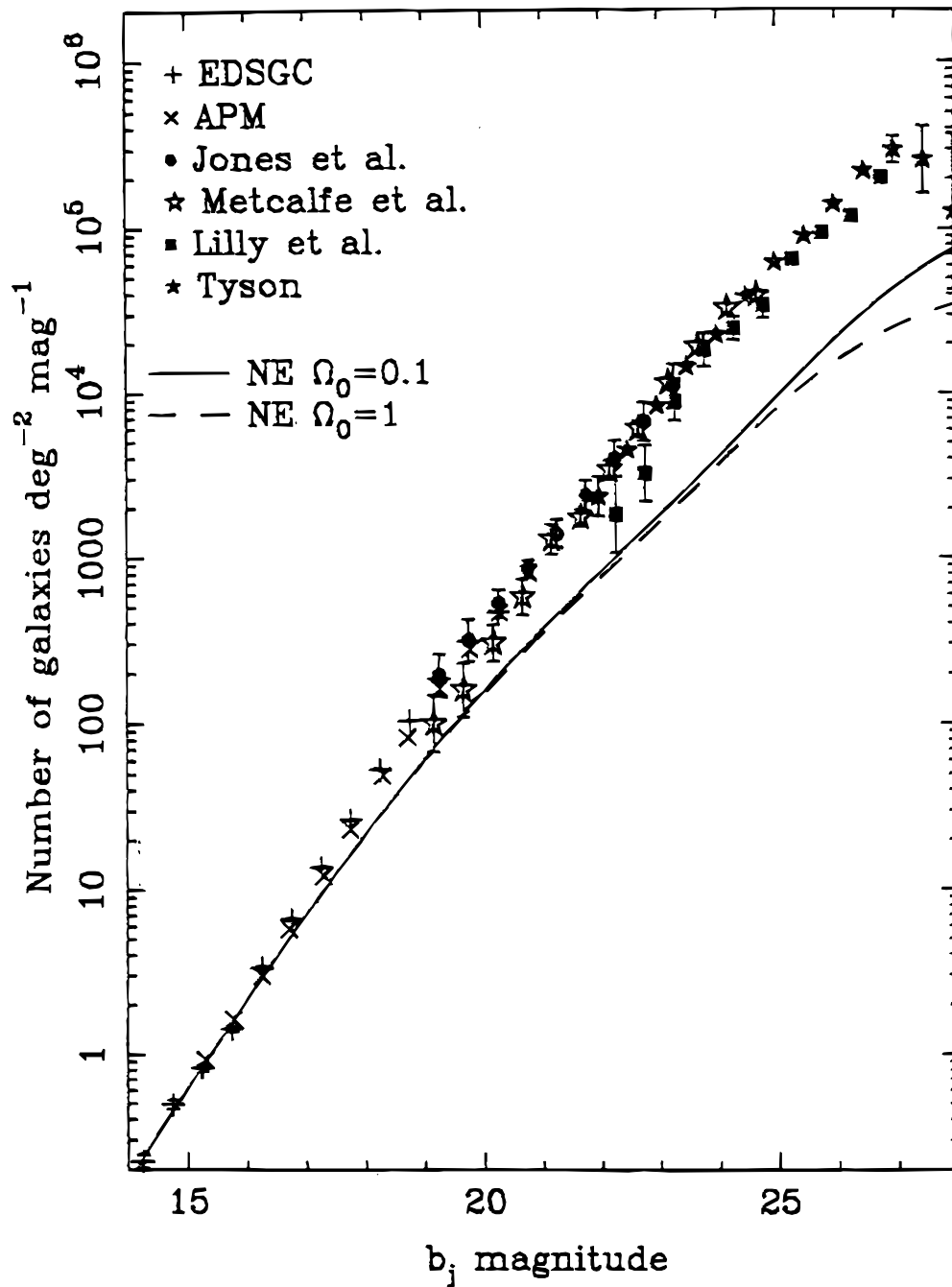


Figure 5.4 - Galaxy number counts as a function of blue magnitude (Glazebrook et al. 1994). Note the excess of faint blue galaxies with respect to the predictions based on the number of nearby galaxies.

principally at UV wavelengths, which can be dominated by small, short-lived populations of hot stars, and is highly sensitive to age, star formation rates, and dust obscuration.

Near-infrared surveys have recently become possible with the availability on ground-based telescopes of near infrared arrays similar to those available on SIRTf. These ground-based studies have revealed a very different picture from that inferred from the visible wavelength studies. A substantial population of luminous galaxies is found in the infrared with homogenous properties implying that most of their star formation occurred at much earlier times (Aragon-Salamanca et al. 1993, Stanford, Eisenhardt, and Dickinson 1995). Dickinson (1995) finds that even in a $z=1.2$ cluster, many galaxies are present with colors

suggesting ages of several billions of years. Figure 5.5 (Djorgovski et al. 1995) shows the deepest number counts to date at K($2.2 \mu\text{m}$) and shows no effect comparable to the excess number of faint blue galaxies. Thus while there has been substantial star formation activity over the last few billion years, as indicated by the blue excess, the bulk of the stellar population as revealed by the near infrared emission has been in place for a much longer time. These studies demonstrate that a sample of galaxies selected at rest wavelengths in the near infrared should provide a much more uniform sample of objects, and a much better estimate of the mass of the observed galaxies, than would a visible light survey. Direct evidence for galaxy formation at an early epoch is afforded by the recent identification – based on ground-based optical data – by Steidel et al (1996) of galaxies in the redshift range $3 < z < 3.5$ at a density on the sky of 0.4 per sq. arcminute.

IRAS observations indicated that much of the star formation in the local Universe occurs in dusty regions within galaxies, often galaxies which appear to be interacting gravitationally or tidally with close companions. The optical and ultraviolet radiation from the newly-formed stars is absorbed by the dust and reradiated at the far infrared wavelengths where IRAS was sensitive. IRAS was able to detect such “starburst galaxies” out to redshifts ~ 0.25 (Soifer et al 1987). SIRTf must be able to observe such objects at much greater redshifts if we are to obtain a complete picture of the cosmic history of star formation.

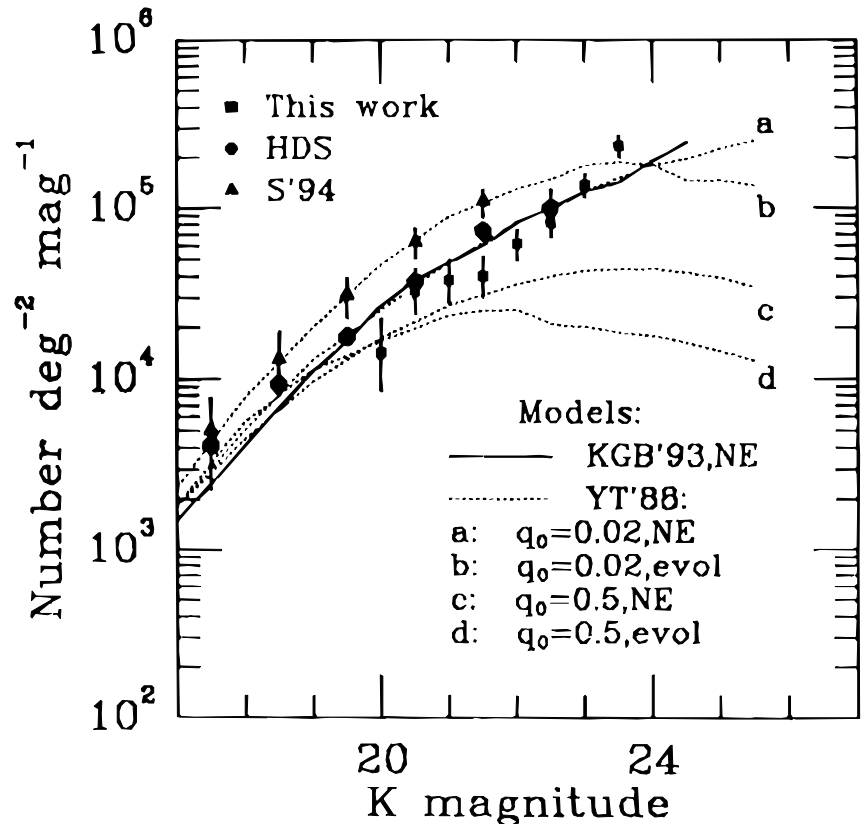


Figure 5.5 - Galaxy number counts as a function of near infrared [$2.2 \mu\text{m}$] magnitude, from Djorgovski et al. (1995). In contrast to Figure 3.4, here the counts agree well with the predictions.

To summarize, our understanding of galaxy evolution now indicates that 1) star formation occurred very soon after the Big Bang; 2) large fractions of the mass of some galaxies was converted into stars by redshifts of 3; and 3) processes for feeding black holes in the centers of galaxies were in place by redshifts of 5; and 4) the maximum in these processes occurred at redshifts of 2-3.

5.2.2. The Extragalactic Background Light

If the numbers of very faint galaxies are large enough, they will “merge” into a diffuse, confusion-limited background³. Thus to reach a full understanding of the history of star and galaxy formation, it will be important to probe the total amount of extragalactic background light (EBL). The amount of EBL – i.e., the accumulated emission from all external galaxies – and its fluctuations from point-to-point can distinguish among different models for the formation and evolution of the galaxy population (Wright, Werner and Rieke 1996).

Recently the DIRBE instrument flown on the COBE mission has made large beam [~42 arcmin] measurements of the infrared sky brightness at wavelengths from 1.2 to 240 μm . This data base is being analyzed to extract the foreground emission from the zodiacal cloud and the galaxy and to search for an extragalactic contribution. These observations should be followed up by SIRTf with pointed observations of DIRBE “dark sky” regions, at sensitivity levels which reach deep into the confusion limit. The combination of the resolved point sources and the residual noise due to source confusion can be analyzed to determine the total point source contribution to the EBL seen by DIRBE in its much larger beam, and to search for any truly diffuse extragalactic component.

5.3 Measurements Required from SIRTf

A SIRTf program to explore the Early Universe should include the following elements:

Program 5.1 - A Deep Survey for Galaxies

Program 5.2 - Determination of Galaxy Redshifts

Program 5.3 - Survey the Dependence of Star Formation on Redshift

Program 5.4 - A Confusion-Limited Survey to Study for the Extragalactic Background Light

Program 5.1 - A Deep Survey for Galaxies

Study of a sample of galaxies reaching to redshifts beyond 3 and reaching down to galaxies of average mass and luminosity is an important part of the exploration of the Early Universe. To produce such a sample, SIRTf must be able to study the starlight of these galaxies at near infrared (3.5–8 μm) wavelengths. This survey should overlap the areas most deeply surveyed by HST and AXAF – most notably the Hubble Deep Field (HDF; Williams et al, 1996). Redshift $z=3$, UV-bright, starforming galaxies have been identified in the HDF, but without rest-frame near infrared

³ The confusion limit is the standard deviation of the flux from individually unresolved and undetected sources within the measuring beam on the sky. It depends on both the size of this beam [and hence on the telescope size] and on the number of sources as a function of flux at low flux levels.

measurements the mass and age of these galaxies remains unknown. Is there an older population of galaxies at $z=3$, in which star formation is already over? Only SIRTf can make the measurements needed to address these questions. A complementary program for studying the Early Universe, focussed on unusual galaxies of very high far infrared luminosity which can serve as beacons for the exploration of even higher redshifts, is described in Section 4.

A SIRTf near infrared survey should determine the galaxy luminosity function, which is the number of galaxies per unit volume per luminosity interval. This is parameterized by a characteristic luminosity L^* , which has the property that the frequency of galaxies fainter than L^* declines slowly with increasing luminosity, while the frequency of galaxies brighter than L^* declines rapidly with increasing luminosity. An L^* galaxy has $L \sim 3 \times 10^{10}$ solar luminosities and is somewhat more luminous than the Milky Way. SIRTf should both construct the galaxy sample and play a role in determining the galaxy redshifts. With redshifts, the galaxies' intrinsic properties are determined, and their luminosity function as a function of redshift can be measured, and, in turn, compared with other distributions such as that of quasars. Measuring the luminosity function as a function of redshift also allows a determination of the evolution with cosmic time of the luminosity and or density of the galaxy population.

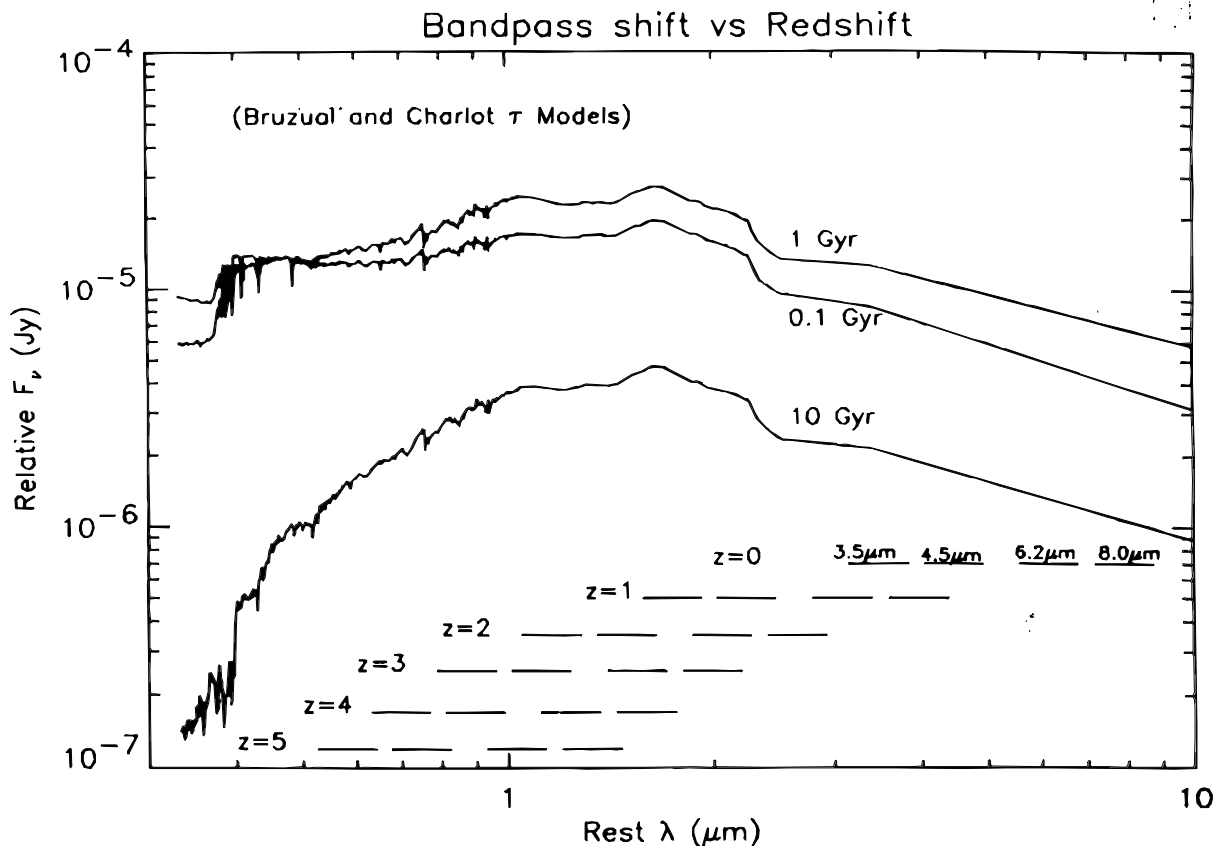


Figure 5.6 - Predicted spectra of galaxies aged 0.1, 1, and 10 Gyr old (Bruzual and Charlot, 1993). Note the early appearance and persistence of the features at 1.6 and 2.3 μm .

In defining the scope of the survey and deriving the measurement requirements, we have assumed a standard, conventional model⁴ to determine brightnesses and integration times. Rest-frame near-IR emission arises from red giant stars over virtually the entire history of a galaxy (see Figure 5.6). Thus a sample based on rest frame near-IR emission will be closely tied to stellar mass, and unbiased by small hot star populations or extinction. A SIRTf survey to test this model and indicate important deviations from the predicted distribution and evolution of the galaxy

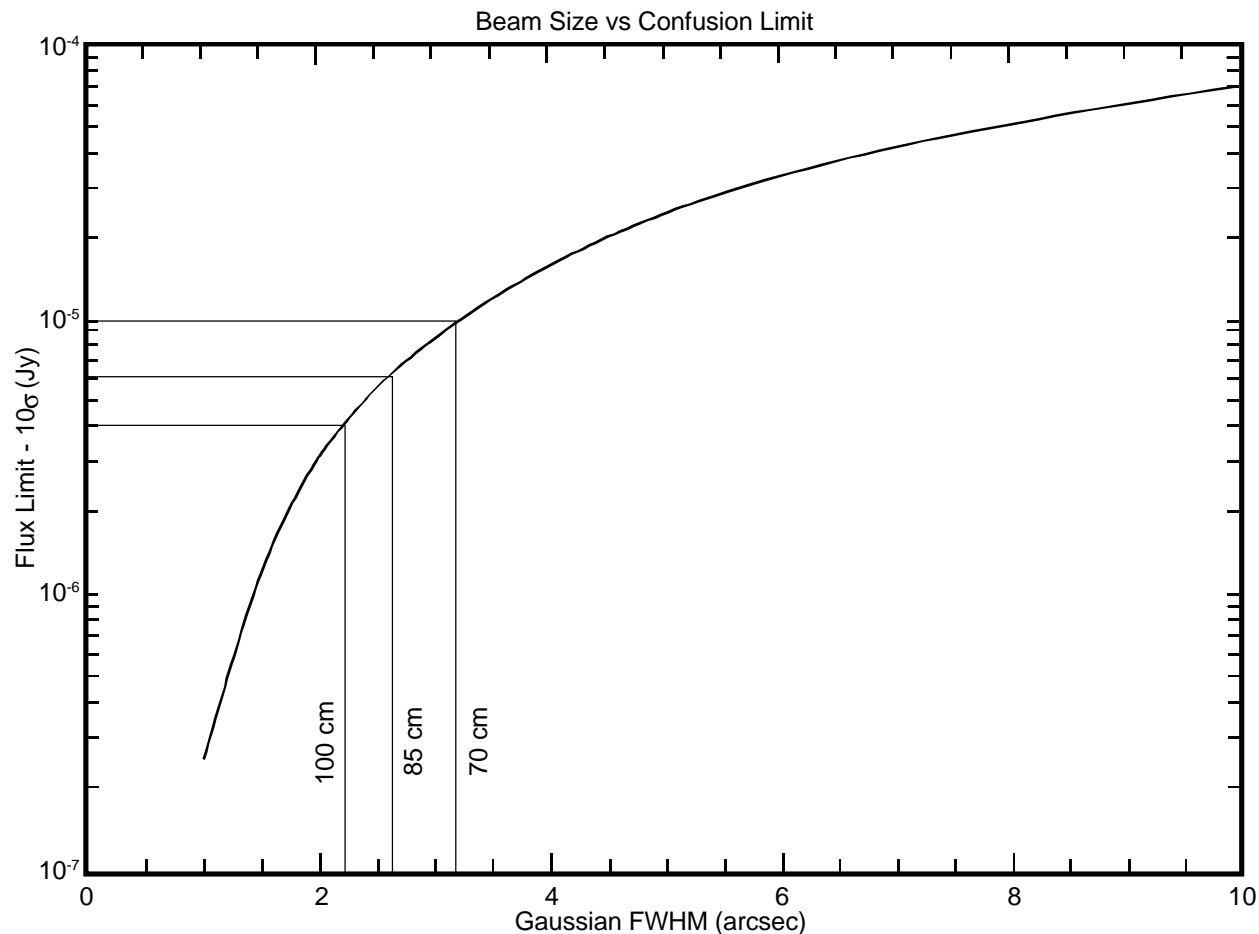


Figure 5.7 - Confusion-limited sensitivity vs. beam size at $8 \mu\text{m}$. The diffraction-limited beam size and sensitivity achievable with telescopes of aperture 70, 85, and 100cm are indicated by the straight lines at the left of the figure. Achieving a sensitivity of $6 \mu\text{Jy}$ (10σ) requires a beam size $\sim < 2.3''$ and hence an aperture of 85cm or greater.

⁴ The model galaxy population was distributed in clusters with redshifts ranging from 0 to 10. Clusters were assumed to form with an exponential distribution of formation times with a mean corresponding to redshift $z=5$ in an $H_0 = 50 \text{ km/sec/Mpc}$, $\Omega = 1$, $\Lambda = 0$ cosmology. The local density of galaxies has been set to 1.33 times the value given by Schechter in order to match the deep K-band counts (Djorgovski et al. 1995). Luminosities and colors evolve using Bruzual (1983) μ -models with a μ that depends on galaxy type. Galaxy spectra are based on the

population must meet the requirements outlined below.

A sample reaching to luminosities below L^* is needed to detect this characteristic signature of the galaxy luminosity function to determine how the galaxy population is evolving; to monitor the rapidly evolving faint end of the luminosity function; and to determine whether mergers are important. It also assures that this survey probes typical galaxies. The sample must extend to $z > 3$, which is beyond the peak in the co-moving density of quasars, to study the coupling between the formation of quasars and the formation of galaxies. We take as a benchmark that the SIRTf survey must be able to measure the flux emitted at $2 \mu\text{m}$ [redshifted to $8 \mu\text{m}$] from an L^* galaxy at $z=3$ to 10σ . The 10σ limit is required so that the photometric redshifts, which depend on flux ratios, can be determined to $\sim 20\%$. From Mobasher et al. (1993) the $2 \mu\text{m}$ (K) magnitude of an L^* galaxy is -25.1 , which corresponds to $6 \mu\text{Jy}$ at $8 \mu\text{m}$ at $z=3$ for $q_0=0.5$ and $H_0=50$. The requirement of reaching a 10σ flux level of $6 \mu\text{Jy}$ at $8 \mu\text{m}$ levies a requirement that the SIRTf primary mirror aperture be at least 85 cm , as a smaller telescope would become confusion-limited at a higher flux level (Figure 5.7), and that the image quality at $8 \mu\text{m}$ not be degraded by aberrations or pointing jitter. This is one of the principal drivers for the aperture size, the image

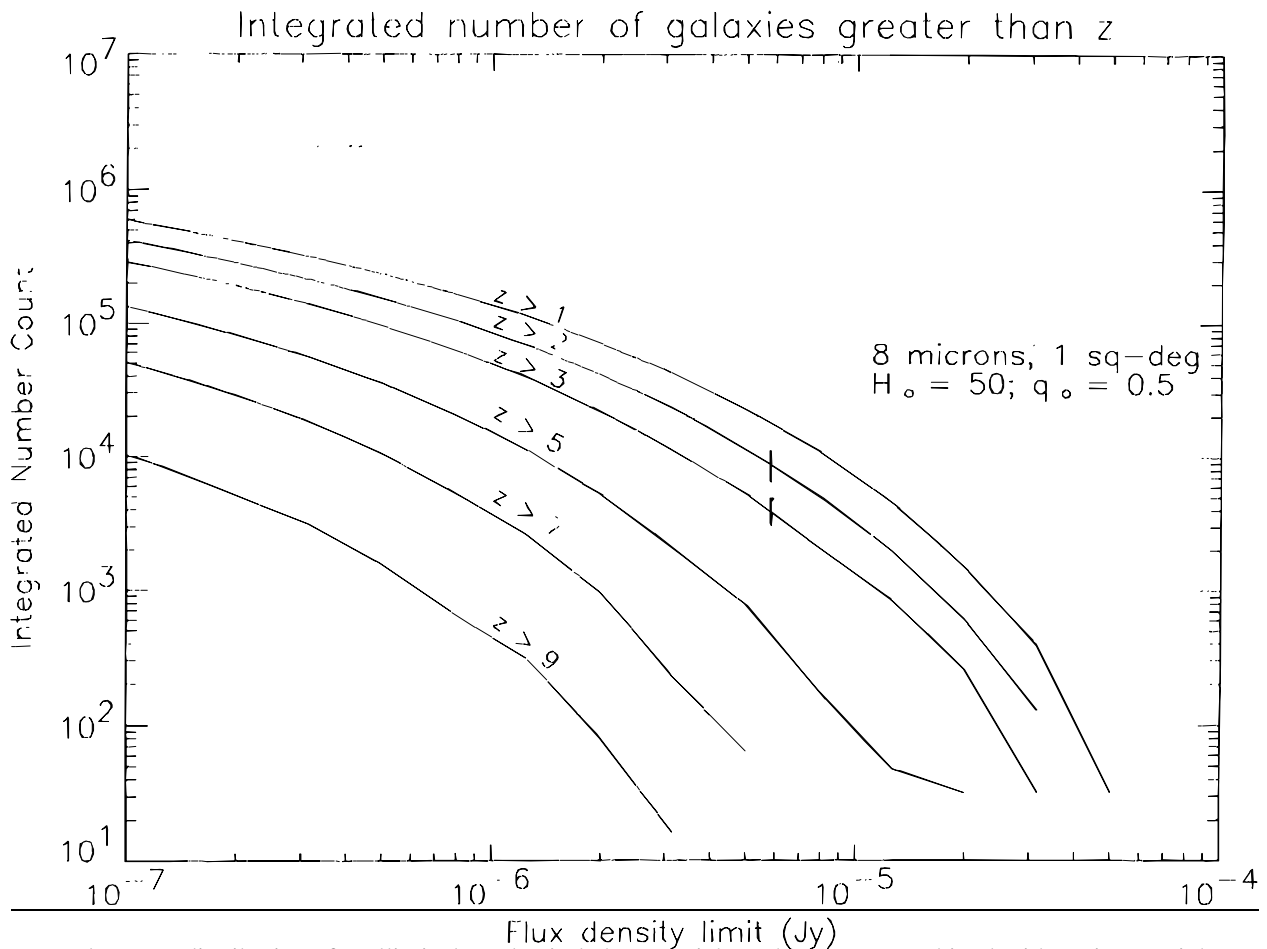


Figure 5.8 Integrated number counts of galaxies as a function of $8 \mu\text{m}$ flux density and redshift. spectral energy distributions for ellipticals and spirals by M. Rieke, which were combined with various weights to match the galaxy models in the literature.

quality, and the pointing stability requirements for SIRTf.

The survey must cover enough area to ensure an adequately sampled luminosity function. Figure 5.8 shows the expected number of galaxies detected at 10σ at $8\ \mu\text{m}$ per square degree as a function of flux and redshift, from calculations by E.L. Wright assuming the standard model of galaxy evolution described above. For $z > 3$, at $6\ \mu\text{Jy}$, this number is $3000/\text{deg}^2$. To measure L^* to a few tenths of a magnitude from a luminosity function requires a sample of at least 200 galaxies (Schechter and Press, 1976). Allowing a factor of 3 for uncertainties in the model due to galaxy evolution, $0.2\ \text{deg}^2$ must be surveyed to $6\ \mu\text{Jy}$ (10σ) at $8\ \mu\text{m}$. Figure 5.8 shows that at $8\ \mu\text{m}$ such a survey would detect 1500 galaxies with $z > 2$, enabling the luminosity function to be constructed as a function of redshift at intervals of 0.25 in redshift. In addition 200 galaxies with $z > 4$ (and $L > L^*$) would be detected.

Program 5.2 - Measure the redshifts of the galaxies in the deep survey

Essentially all redshifts for distant galaxies have been obtained from measurements of emission lines such as [OII] 3727 and Lyman alpha, or of absorption features seen against a strong ultraviolet continuum. Steidel et al. (1996a) have demonstrated the effectiveness of a 3 color system in measuring photometric redshifts using the Lyman break feature for UV-bright galaxies with $3 < z < 3.4$, and by using the four HDF filters have extended the range to $2 < z < 4.5$ (Steidel et al. 1996b). But all these approaches are biased towards blue star-forming galaxies. To enable construction of the true luminosity function of galaxies vs. redshift, a technique for measuring redshifts for ALL galaxies in the sample is necessary. The $1.6\ \mu\text{m}$ peak, which (unlike the Lyman break) is present in both actively star forming and quiescent galaxies at all epochs after the first few tens of millions of years of star formation (Figure 5.6), is a suitable feature for estimating redshift. Figure 5.9, which is derived from the same simulation used for Figure 5.8, illustrates that the $1.6\ \mu\text{m}$ feature creates a well-defined correlation between redshift and flux ratios in the 3 to $8\ \mu\text{m}$ range, enabling the determination of photometric redshifts for galaxies of redshift from $z < 1$ to $z > 4$. Work on the HDF illustrates that four wavelength

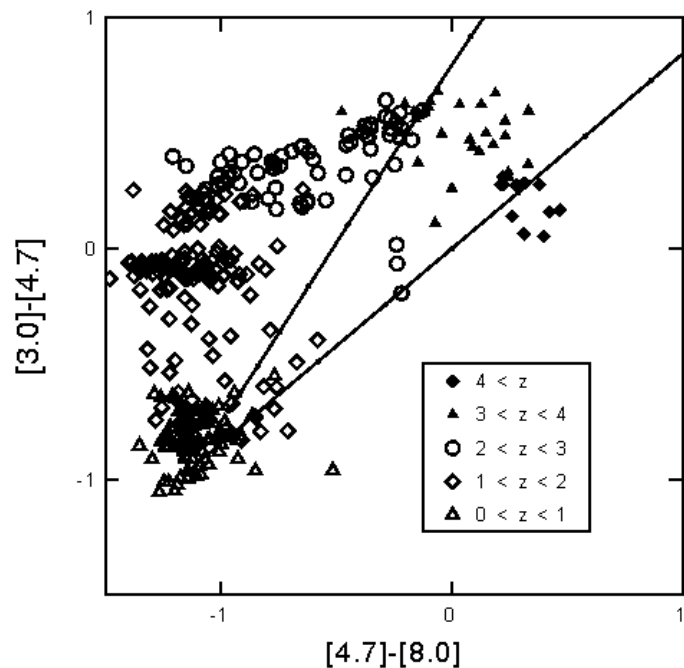


Figure 5.9 - Two color plot of galaxies identified in a simulated SIRTf deep survey. Note that the position of a galaxy in this plot correlates extremely well with the galaxy's redshift, which is known from the input to the simulation. The upper solid line shows the locus of blackbodies of various temperatures (i.e. stars), while the lower line corresponds to power law continua.

bands provide greater robustness and sensitivity over a large redshift range than do 3 bands. Thus redshift determinations for a complete sample require observations 3.5, 4.5, 6.3, and 8 μm .

Because photometric redshifts will always be considered less reliable than those obtained spectroscopically, it will be important to obtain spectral redshifts for a convincing subsample of objects. Thus the detailed strategy for this and other SIRTf surveys should exploit opportunities resulting from explorations in other wavelength bands. For example, if a portion of this survey overlaps with the region of sky studied in the Hubble Deep Field survey, redshifts may be available for those objects out to $z > \sim 2$ from ground and space-based spectroscopic follow-up. These results could be used to validate the efficacy of the photometric redshift determinations.

In addition, at the very earliest stages of formation (the first 10 million years), the 1.6 μm bump is not expected to be prominent in the spectrum of a galaxy, because the red giant and supergiant stars which exhibit this feature are produced by the evolution of the first generation of stars. The SIRTf deep survey may thus identify a number of candidate protogalaxies by the absence of this 1.6 μm feature. However, galaxies this young may have strong optical and UV emission lines characteristic of massive young stars and thus be susceptible to spectroscopy and high resolution imaging with HST or groundbased near IR adaptive optics. If such objects are heavily obscured, their spectra should show dust emission signatures such as the 3.3 μm PAH feature, or the 10 μm silicate feature, – redshifted to longer wavelengths – and SIRTf spectroscopy could determine the redshift, as discussed in Section 4. This type of follow on from SIRTf will require that the positions of targets from SIRTf's deep surveys be reconstructed with sub arcsecond accuracy to permit placement of the objects on the spectrograph slits; alternatively, the galaxies may be acquired by the use of a pickup mode in the spectrograph.

Program 5.3 - Survey the dependence of star formation on redshift.

HST surveys are sensitive to galaxies with recent star formation but little obscuration by dust. Near infrared surveys, on the other hand, will find galaxies with a significant fraction of their total emission from evolved stars. Neither approach, however, will be sensitive to galaxies undergoing massive, but dust-embedded bursts of star formation, since the dust shrouding such regions will absorb the bright ultraviolet emission from new stars and reradiate it in the far infrared. As IRAS showed, such “starburst” galaxies are numerous nearby, and the bulk of star formation in the local Universe probably occurs in such dust-embedded environments, both in galactic nuclei and in dust-and-gas rich spiral arms which define the morphology of spiral galaxies.

SIRTf, with much greater sensitivity than IRAS, should conduct sensitive surveys in the far infrared to detect and characterize the high-redshift counterparts of the IRAS galaxies. In this way SIRTf can investigate changes in the star formation rate as a function of redshift and relate them to the evolution of other characteristics of the galaxy population, including those discovered in the near infrared survey described above. For example, IRAS' results suggest that, locally, starburst activity is triggered by collisions or interactions between galaxies. Because the distance between galaxies was less at earlier epochs, collisions ought to have been more frequent. If this line of reasoning is correct, it leads to predictions about the observed number density of galaxies at various flux levels (Figure 5.10) which can be tested with observations such as those described below.

Figure 5.10 shows predicted counts at $70\mu\text{m}$ of galaxies per unit solid angle on the sky as a function of $70\mu\text{m}$ brightness. The curves are parameterized such that in a non-expanding, non-evolving universe the counts would be a horizontal line. The “no evolution” line corresponds to an expanding universe in which the density of starburst galaxies is constant, while the “evolving” model predicts more fainter galaxies because of an increased rate of galaxy collisions at earlier times. SIRTf can distinguish among these and other models if it is capable of achieving the indicated sensitivity level at $70\mu\text{m}$.

We adopt as a goal to survey an adequate area on the sky to provide a volume between $z=1.5$ and $z=2.5$ which is equivalent to the volume surveyed by IRAS. Our sensitivity goal is to survey to a luminosity that, assuming evolution as $(1+z)^2$, corresponds to $10^{11} L_{\odot}$ at the present epoch, since this luminosity extends well into the starburst regime. Adopting a cosmology with $H_0 = 75 \text{ km/s/Mpc}$ and $q_0 = 0.5$, the area to be surveyed is ~ 1 sq degree. However, to provide an adequate context for the confusion-limited survey described below, we propose a survey of ~ 5 sq degree. This survey should be at three wavelengths beyond $20\mu\text{m}$ to allow sorting of the objects according to far infrared color temperature, and it should be coordinated with shorter wavelength surveys from SIRTf as well as with ground- and space-based surveys across this electromagnetic spectrum, since a major effort will be needed to acquire enough information to understand the results of this survey. The required sensitivity (10σ) for this survey are estimated to be 0.4 mJy at $24\mu\text{m}$, 2 mJy at $70 \mu\text{m}$ and 20 mJy at $160 \mu\text{m}$.

A second survey of roughly 50 square degrees to one-third the depth of the small-scale survey would provide a comparison sample of galaxies from $z=0.2$ to $z=1.5$ and would cover

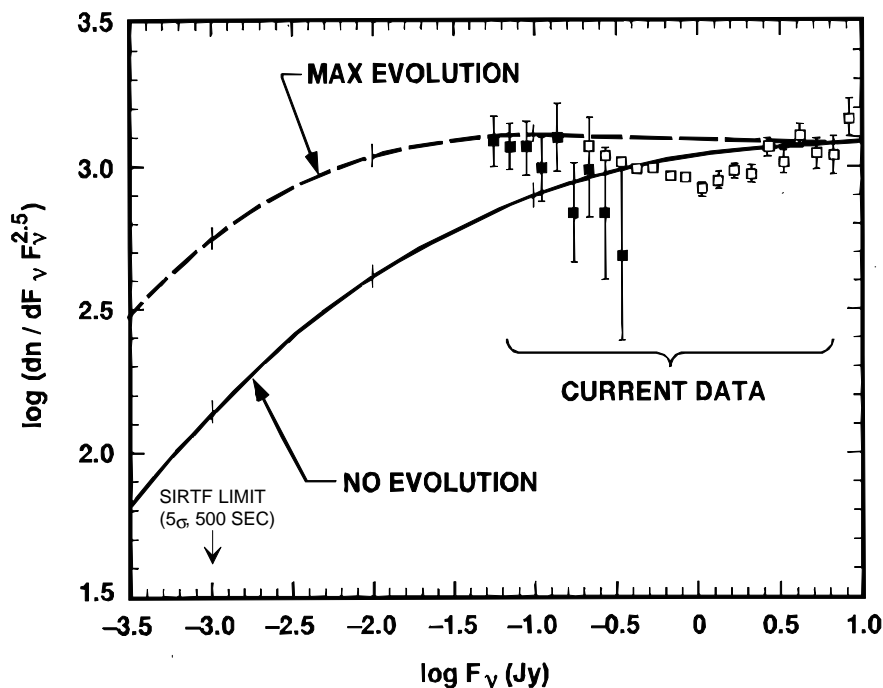


Fig. 5.10 Galaxy number counts at $70 \mu\text{m}$ (from Hacking & Soifer, 1991)

similar comoving volumes to IRAS and to the deep SIRTf survey. This large-area survey would reach sensitivities of 1 mJy at $24\mu\text{m}$, 5 mJy at $70\mu\text{m}$, and 60 mJy at $160\mu\text{m}$.

These two surveys together would provide the data needed to test the models illustrated in Figure 5.10 above. Note that the prime data required for both of these surveys at $70\mu\text{m}$ – and a good deal of the required follow on observations – could be obtained in the extensive $70\mu\text{m}$ survey described

as Program 4.1. This survey would be optimized for the detection and identification of very luminous objects at redshifts $z > 5$, but of necessity would also detect and identify, spectroscopically, many less luminous objects at lower redshifts. Thus a SIRTf survey designed for a particular application may in many cases serve multiple scientific needs.

Survey 3 would cover up to one square degree with 10σ sensitivity ~ 0.5 mJy at $70 \mu\text{m}$, 15 mJy at $160 \mu\text{m}$ and 0.04 mJy at $25 \mu\text{m}$. It would be confusion limited to measure the extragalactic background, and it is described in more detail in the next section.

Program 5.4 - A Confusion-Limited Survey and a Search for the Extragalactic Background Light

A confusion-limited survey will achieve the highest sensitivity attainable from a telescope of given size. For SIRTf, which should be confusion-limited at high galactic latitude by distant galaxies, the survey would trace the galaxy luminosity function [by permitting modelling of the confusion noise] to levels fainter than the faintest clearly distinguishable source[s]. The results of this survey could have profound implications for our understanding of galaxy formation and the early Universe. In addition, an extrapolation of this luminosity function, compared with the sky brightness measured by COBE, could be used to search for a diffuse component to the extragalactic background light. Because such a survey would reach the ultimate sensitivity limits accessible to SIRTf, it is a measurement of fundamental importance for the mission. It would have to be carried out at high galactic latitude and high ecliptic latitude in a region of low infrared background.

Data from the DIRBE experiment on COBE shows that the contrast of any Extragalactic Background Light (EBL) relative to the foreground zodiacal light is potentially greater at $3.5 \mu\text{m}$ than at wavelengths where the EBL might be observed from the ground, so a confusion-limited SIRTf survey at $3.5 \mu\text{m}$ will be an important companion to the $8 \mu\text{m}$ survey described earlier. Extending the survey to the far infrared would allow a similar analysis of the population of infrared-luminous, dusty, starburst galaxies which will complement the 3.5 and $8 \mu\text{m}$ surveys of galaxies dominated by starlight. To be of greatest use, these surveys should all overlap on the sky and include the same 0.2 deg^2 encompassed by the deep $8 \mu\text{m}$ survey discussed earlier. Surveying one square degree in the far infrared assures that a volume of the distant ($z > 2.5$) Universe equivalent to that mapped out locally by IRAS is included. It would provide the deepest look at the far infrared sky for the foreseeable future. At least part of the sky area covered in this very deep survey should be covered as well in deep ground-based and space-based surveys across the electromagnetic spectrum. The IR-brightest objects, and especially those objects that can be seen only by SIRTf, will be prime objects for follow-up observations with the spectrograph.

The SIRTf aperture size must be at least 85 cm to meet the goals for galaxy formation described above. For this size telescope, the 10σ confusion limit at $70(160) \mu\text{m}$ is expected to be $0.5(15)$ mJy. A 1 sq degree area would contain about 25000 galaxies brighter than this limit. At $3.5 \mu\text{m}$, the 10σ confusion limit is approximately 5 μJy , and the 1 deg^2 area would contain tens of thousands of galaxies. This flux level at $3.5 \mu\text{m}$ corresponds approximately to the turnover in the counts where the contribution of faint galaxies to the total brightness starts to converge (Wright et al, 1996) and is thus of particular importance for studying the EBL. The object of the EBL investigation is in fact to measure the confusion noise, so that sensitivity requirement (see Table

5.1) is to have the photon noise well below the confusion noise. Very long integrations would be required to achieve these sensitivity levels at 8 and 24 μ m; thus accomplishing this program in a reasonable time will make full use of the large-format arrays to be flown on SIRTf.

Measurements of total sky brightness, e.g. for comparison with the COBE large beam, are an important part of the search for the EBL. These absolute measurements lead to the need for a way to blank off SIRTf's cameras to permit a measurement of the instrumental offset with zero flux falling on the detector. The presence on SIRTf of a shutter in the short wavelength camera and a scan mirror in the long wavelength camera, each of which might be needed for other purposes, would facilitate these absolute measurements.

Table 5.1 - Science Requirements for the Early Universe Program

Program	Wavelength Range (μm)	Sensitivity required	Spectral Resolution	Spatial Resolution	# of Targets	Comments
5.1 - L* Galaxies at $z > 3$	8 μm	6 μJy , 10σ	0.25	~2" images	0.2 sq. degrees - expect 600 L* galaxies at $z > 3$	Reach confusion limit at 8 μm
5.2 - Redshifts for Galaxies from 5.1	3.5, 4.5, 6.3 μm	6 μJy , 10σ , in each band	0.25	~2"	0.2 sq degrees - identical area to that measured in 5.1	Use flux ratios for photometric redshift
5.3 - Dependence of Star Formation on Redshift (2 part program)	24, 70, 160 μm	a) 1/5/60mJy (10σ) @ 24/70/160 μm b) 0.4/2/20mJy (10σ) @ 24/70/160 μm	~0.25	7" @ 24 μm , 15" @ 70 μm , 40" at 160 μm	a) 50 sq degrees b) 5 sq degrees	a)= IRAS volume at $0.2 < z < 1.5$ b)= IRAS volume at $1.5 < z < 2.5$ Surveys may overlap with program 4.1
5.4 - Confusion Limited Survey - Objectives are Extragalactic Background and Galaxy Evolution	3.5, 8, 24, 70, 160 μm	Photon noise to be less than 0.4, 0.6, 4, 60, 1500 μJy per point source beam at 3.5, 8, 24, 70 μm , 160 μm to reach deep into confusion limit	~0.25	~2" @ 3.5 μm , ~2" @ 8 μm ; ~7" @ 30 μm ; ~15" @ 70 μm ; 40" @ 160 μm	Cover at least 0.2 sq degree. Use 3.5, 8 μm data from 5.1 and 5.2	Need ability to make absolute sky brightness measurements.

Appendix A

Astrophysics Missions and Programs Complementary to SIRTf

This appendix describes very briefly the astrophysics missions and programs discussed in the text, with emphasis on their relationship to SIRTf.

AXAF - Advanced X-Ray Astrophysics Facility (1998) - AXAF is the X-Ray component of the Great Observatories program (see discussion under HST below). The arguments for complementarity and overlap given for SIRTf and HST apply to SIRTf and AXAF as well. The scientific areas where AXAF and HST are likely to be most complementary are in the study of Active Galactic Nuclei, the Early Universe, and Young Stellar Objects.

COBE - Cosmic Background Explorer (1989). COBE was dedicated to the study of the infrared and microwave background radiation. Its measurements of the spectrum and spatial structure of the microwave background are of profound astrophysical importance. The DIRBE experiment on COBE measured the infrared background from $<3 \mu\text{m}$ to beyond $200 \mu\text{m}$ with ~ 30 arcmin resolution. COBE provides precise measurements of the foreground zodiacal emission through which SIRTf observes the Universe. In addition, COBE will provide estimates of the total brightness of the extragalactic background radiation in the infrared which can be compared with the integrated contribution of the point sources seen by SIRTf.

HST - Hubble Space Telescope (1990). HST is NASA's premiere facility for optical and ultraviolet space astronomy, and its capabilities were extended out to $2.5 \mu\text{m}$ in the near infrared with the addition of the NICMOS instrument in early 1997. HST and SIRTf, together with AXAF (see above) and the Compton Gamma Ray Observatory, make up NASA's family of Great Observatories. HST will provide high angular resolution images - as well as optical and ultraviolet spectra - of many of the objects to be studied by SIRTf. Correspondingly, SIRTf observations of targets studied by HST, such as the Hubble Deep Field, will be of great scientific interest. Both facilities will explore the Early Universe to great depth. There is thus a great deal of scientific complementarity between HST and SIRTf, and it is very important to launch SIRTf in 2002 - earlier if possible - while HST is still fully functional, in order to maximize the time available for coordinated and follow-on programs.

IRAS - Infrared Astronomical Satellite (1983). The first major cryogenic mission for infrared astronomy. IRAS surveyed the entire sky at 12, 25, 60, and $100 \mu\text{m}$ with a 60 cm aperture telescope and spatial resolution several arcmin. It established the scientific and technical basis for subsequent missions, including SIRTf.

ISO - Infrared Space Observatory (1995) - ISO is the first pointed, multi-instrument, cryogenic observatory for infrared astronomy from space. It provides major advances in sensitivity and in spatial and spectral resolution over IRAS and covers the wavelength range ~ 3 - $200 \mu\text{m}$, using a 60 cm diameter telescope. ISO will carry out the first spectroscopic and imaging studies of many of the phenomena discovered by IRAS and define new questions to be explored

by SIRTf. ISO's instruments use single detectors or small detector arrays, in contrast to the much larger arrays available for SIRTf.

SDSS - Sloan Digital Sky Survey (1997) - The SDSS will execute an unbiased survey of about one-quarter of the sky at visual wavelengths using a 2.5-m telescope and a large number of large-format CCD detectors. It will provide imaging, positions and photometry of objects as faint as 23rd magnitude, including about fifty million galaxies, a somewhat larger number of stars, and about one million quasars. Spectra will be obtained of the one million brightest galaxies and the 100,000 brightest quasars. Choosing SIRTf's large area surveys to coincide with areas already included in the SDSS assures that much of the follow-on of the SIRTf programs will effectively have been done beforehand.

SOFIA - Stratospheric Observatory for Infrared Astronomy (2002). SOFIA will carry a ~2.5m diameter telescope in a modified 747 aircraft into the lower stratosphere for infrared and submillimeter astronomical investigations. SOFIA will be scientifically complementary to SIRTf - As a warm telescope, it will not approach SIRTf's sensitivity for imaging or spectroscopy, and even at stratospheric altitudes the Earth's atmosphere is selectively opaque at the wavelengths of particularly important molecular and atomic species. However, SOFIA will provide somewhat higher spatial resolution - and considerably higher spectral resolution - than SIRTf and will also carry out observations at the submillimeter wavelengths not covered by SIRTf.

2MASS - Two-Micron All-Sky Survey (1997-). 2-MASS will provide a survey of the entire sky at wavelengths of 1.2, 1.6, and 2.2 μm . It will provide valuable near infrared flux measurements and images of the galaxies and stars to be observed by SIRTf. SIRTf and 2-MASS data together can be used to select unusual objects for further study, e.g. by comparing SIRTf's 3.5-to-8 μm data with the 2-MASS data base. This will be particularly valuable for SIRTf's brown dwarf and young stellar object programs.

VLA - Very Large Array (1981) - The VLA is a multi-antenna radio telescope which can achieve both very high sensitivity and very high spatial resolution. SIRTf and the VLA can be used together in studies of ultraluminous infrared galaxies and active galactic nuclei.

WIRE - Wide Field Infrared Explorer (1998). WIRE is a Small Explorer mission dedicated to the study of the evolution of the starburst galaxy population. It will carry a 30 cm telescope and image a few hundred degrees of high galactic latitude sky at 12 and 25 μm , making the first use in space of large format arrays of the type to be used on SIRTf. WIRE's scientific results will be extremely important in the planning of SIRTf's studies of infrared-luminous galaxies, and SIRTf's spectroscopic investigations will include study of objects identified by WIRE as being of particular interest.

References

- Adams, F., Lada, C.J., and Shu, F.H. 1987, *ApJ*, 312, 788.
- Adams, F. and Laughlin, G. 1996, *ApJ*, 468, 586
- Alcock, C. et al. 1993, *Nature*, 365, 621.
- Alcock, C. et al. 1996, *ApJ*, 461, 84.
- Allard, F., Hauschildt, P., Baraffe, I. and Chabrier, G. 1996, *ApJ*, 465, L123.
- Aragon-Salamanca, A., Ellis, R.S., Couch, W.J., and Carter, D. 1993, *MNRAS*, 262, 764.
- Aumann, H.H., and Good, J.C. 1990, *ApJ*, 350, 408.
- Backman, D., Das Gupta, A., and Stencel, R.E. 1995, *ApJ*, 450, L75.
- Backman, D.E., and Paresce, F. 1993, in *Protostars and Planets III*, 1253.
- Bahcall, J. N., Schmidt, M. & Soneira, R. M. 1982, *ApJ*, 258, L23
- Bahcall, J., Flynn, C., Gould, A. and Kirhakos, S. 1994, *ApJ* 435, L51.
- Bahcall, J.N., Kirhakos, S., and Schneider, D.P. 1995, *ApJ*, 450, 486.
- Basri, G., Marcy, G.W., and Graham, J.R. 1996, *ApJ*, 458, 600.
- Basu, S., and Rana, N. C. 1992, *ApJ*, 393, 373
- Bliek, N. S., van der, Prusti, T., & Waters, L. B. F. M. 1994, *A&A*, 285, 229
- Bruzual, G. 1983, *ApJ* 273, 105.
- Bruzual, G., and Charlot, S. 1993, *ApJ*, 405, 538.
- Burrows, A., Hubbard, W. B., Saumon, D. & Lunine, J. I. 1993, *ApJ*, 406, 159
- Burrows, A. et al. 1996, in “Sources and Detection of Dark Matter in the Universe”, ed. D.Sanders et al.
- Butler, P., and Marcy, G. 1996, *ApJ*, 464, L153.
- Campins, H. et al. 1987, *Astron. Astrophys.*, 187, 601.
- Chabrier, G. et al. 1996, *ApJ*, 468, L21.
- Cochran, A., Levison, J.P., Stern, S.A. and Duncan, M. 1995, *ApJ*, 455, 342.
- Cutri, R.M., et al. 1994, *ApJ*, 424, L65.
- Dahn, C., Liebert, J., Harris, H.C., and Guetter, H. 1994, in *The Bottom of the Main Sequence and Beyond*, C. Tinney (ed), p. 239.
- De Paolis, F., et al. 1996, *ApJ*, 470, 493.
- Dickinson, M.E. 1995, in *Lecture Notes in Physics, #463, Galaxies in the Young Universe*, ed. H. Hippelein, K. Meisenheimer, and H.-J. Roser (Berlin: Springer), 144.
- Djorgovski, S. et al. 1995, *ApJ*, 438, L13
- Eisenhardt, P. et al. 1996, *ApJ*, 461, 72.

- Evans, N. W. & Jijina, J. 1994, MNRAS, 267, L21
- Fekel, F. C., & Bopp, B. W. 1993, ApJL, 419, L89
- Glazebrook, K., Peacock, J.A., Collins, C.A., and Miller, L. 1994, MNRAS 266, 65
- Gould, A., 1994, ApJ Letters, 421, L75.
- Graff, D. and Freese, K. 1996, ApJ, 467, L65.
- Gregorio-Hetem, J., Lepine, J. R. D., Quast, G. R., Torres, C. A. O., & de la Reza, R. 1992, AJ, 103, 549.
- Hacking, P.B., and Soifer, B.T. 1991, ApJ, 367, L49.
- Hammel, H.B., et al. 1987, Astron. Astrophys., 187, 665.
- Han, C. and Gould, A. 1996, ApJ 467, 540.
- Hanner, M.S., et al. 1987, Astron. Astrophys., 187, 653.
- Hanner, M., Tokunaga, A.T., and Geballe, T. 1992, ApJ, 395, L111.
- Hillenbrand, L., et al. 1992, ApJ, 397, 613.
- Irvine, W., and Pollack, J. 1968, Icarus, 8, 324.
- Jetzer, P. 1994, ApJ,432, L43 (also ApJ, 438, L49).
- Jura, M., Zuckerman, B., Becklin, E. E., & Smith, R. C. 1993, ApJL, 418, L37
- Kenyon, S., et al. 1990, AJ, 99, 869.
- Knacke, R.F., et al. 1993, ApJ, 418, 440.
- Kormendy, J., et al. 1996, ApJ, 459, L57.
- Lada, C.J., Young, E.T., and Greene, T.P. 1993, ApJ, 408, 471.
- Lagage, P.O., and Pantin, E. 1994, Nature, 369, 628.
- Lanz, T., Heap, S., & Hubeny, I. 1995, ApJL, 447, L41
- Lutz, D., et al. 1996, Astron. Astrophys., 99, 869.
- Luu, J., and Jewett, D. 1996, Ast. Soc. Pacific Conf. Proc., 107, 245.
- Magazzu, A., Martin, E.L., and Rebolo, R. 1993, ApJ, 404, L17.
- Marcy, G., and Butler, P. 1996, ApJ, 464, L147.
- Marley, M.S., et al. 1996, Science, 272, 1919.
- Martin, E., Rebolo, R., Zapatero-Osorio, M. 1996, ApJ 469, 706.
- Mayor, M., and Queloz, D. 1995, Nature, 378, 355.
- Mobasher, B., Sharples, R.M., and Ellis, R.S. 1993, MNRAS, 263, 560.
- Mukai, T., and Koike, C. 1990, Icarus, 87, 180.
- Nakajima, T., et al. 1995, Nature 378, 463.

- Nelson, L. A., Rappaport, S. A. & Joss, P. C. 1986, ApJ, 311, 226
- Neufeld, D.A., and Hollenbach, D.J. 1994, ApJ, 428, 170.
- Neufeld, D., and Melnick, G.J. 1987, ApJ, 322, 266.
- Omont, A. et al. 1990, ApJ, 355, L27.
- Rebolo, R., Martin, E.L. and Magazzu, A. 1992, ApJ, 389, L83.
- Rebolo, R., Zapatero-Osorio, M., and Martin, E. 1995, Nature, 377, 129.
- Rieke, M., 1996. Personal communication.
- Salisbury, J.W., Daria, D.M., and Jarosewitch, E. 1990, in “Reports of Planetary Geology and Geophysics Program”, (NASA), 262.
- Salpeter, E. 1992, ApJ 393, 258.
- Sanders, D. et al. 1987, ApJ, 325, 74.
- Scalo, J. 1986, Fund. Cos. Phys., 11, 144
- Schechter, P., and Press, W.H. 1976, ApJ, 203, 557.
- Schmidt, M., Schneider, D.P., and Gunn, J.E. 1995, AJ, 110, 68
- Schutte, W. et al. 1990, ApJ, 360, 577.
- Shiba, H., et al. 1993, ApJS, 89, 299.
- Soifer, B.T., Neugebauer, G., and Houck, J.R. 1987, Ann. Rev. Astron. Astrophys, 25, 187.
- Stanford, S.A., Eisenhardt, P.R.M., and Dickinson, D. 1995, ApJ, 450, 512.
- Stauffer, J., Hamilton, D., Probst, R., Rieke, G. and Mateo, M.
1989, ApJ 344, L21.
- Stauffer, J., Hamilton, D., and Probst, R. 1994, AJ, 108, 155.
- Stauffer, J. R., Hartmann, L. W., & Navascues, D. B. y 1995, ApJ, 454, 910
- Steidel, C., et al. 1996a, ApJ, 462, L17.
- Steidel, C., et al. 1996b, AJ, 112, 352.
- Telesco, C., et al. 1988, Nature, 335, 51.
- Tinney, C. G. 1993, ApJ, 414, 279.
- Voit, G.M. 1992, ApJ, 399, 495.
- Weissman, P. 1995, Ann. Rev. Astron. Astrophys., 33, 337.
- Williams, D.M. , et al. 1996, ApJ, 464, 268.
- Williams, R.E., et al. 1996, AJ, 112, 1335.
- Wright, E.L., Werner, M.W., and Rieke, G.H. 1996, in “Unveiling the Cosmic Infrared Background”, (AIP Conf. Proc. 346), ed. E. Dwek, 278.